Universidade de Aveiro Departamento de Biologia
2015

Rui Machado Gonçalves

Functional analysis of String/CDC25 phosphatase in post-mitotic neurons

Análise funcional da fosfatase String/CDC25 em neurónios pós-mitóticos

Declaração

Declaro que este relatório é integralmente da minha autoria, estando devidamente referenciadas as fontes e obras consultadas, bem como identificadas de modo claro as citações dessas obras. Não contém, por isso, qualquer tipo de plágio quer de textos publicados, qualquer que seja o meio dessa publicação, incluindo meios eletrónicos, quer de trabalhos académicos.

Universidade de Aveiro Departamento de Biologia
2015

Rui Machado Gonçalves

Functional analysis of String/CDC25 phosphatase in post-mitotic neurons

Análise funcional da fosfatase String/CDC25 em neurónios pós-mitóticos

Dissertação apresentada à Universidade de Aveiro para cumprimento dos requisitos necessários à obtenção do grau de Mestre em Biologia Molecular e Celular, realizada sob a orientação científica da Doutora Carla Sofia da Silva Lopes, Investigadora auxiliar do Instituto de Biologia Molecular e Celular (IBMC), e da Doutora Maria Paula Polónia Gonçalves, Professora associada do Departamento de Biologia da Universidade de Aveiro.

This work was financially supported by national funds through FCT – Fundação para a Ciência e a Tecnologia/MEC – Ministério da Educação e Ciência and when applicable co-funded by FEDER funds within the partnership agreement PT2020 related with the research unit number 4293.

O júri

presidente	Doutora Maria de Lourdes Gomes Pereira Professor Associado com agregação do Departamento de Biologia da Universidade de Aveiro
arguente	Doutora Catarina Alexandra Brás Pereira Investigador Pós-Doutoramento do Instituto Gulbenkian de Ciência (IGC)
orientador	Doutora Carla Sofia da Silva Lopes Investigador auxiliar do Instituto de Biologia Molecular e Celular (IBMC)

Agradecimentos

E depois de um ano intenso, repleto de novos desafios e emoções à mistura, chegou a hora de agradecer a todas as pessoas que de algum modo contribuíram para que mais uma etapa da minha vida se concluísse:

- à minha orientadora, Carla Lopes, obrigado por toda a dedicação e atenção prestados, por todos os conhecimentos transmitidos ao longo de todo o ano. Obrigado por me ter apresentado "o mundo da *Drosophila*" e o quão dinâmico, fantástico e enriquecedor é fazer investigação com este modelo. Ser integrado no seu grupo de investigação foi sem sombra de dúvidas a escolha mais certeira! Foi imensamente gratificante em vários níveis, não só científico mas também pessoal.

- à minha co-orientadora, Paula Gonçalves, que tem acompanhado mais de perto o meu percurso científico nos últimos tempos. Não podia deixar de lhe agradecer por todo o apoio e votos de confiança que tem depositado em mim, e que também tiveram ótimas repercussões no meu crescimento científico.

- aos meus Pais e Irmão, pelo apoio incondicional, por estarem sempre presentes e por se esforçarem tanto para me proporcionar um futuro melhor. Sem vocês nada disto teria sido possível!!

- à Débora, pela amizade, pelos fantásticos e memoráveis momentos que marcaram o meu primeiro ano de Mestrado!! Obrigado por tudo, pelo apoio e confiança, mesmo que agora estando mais afastados.

- à Diana, que entrou comigo nesta aventura! E agora vou ter de ser bem concreto para não escrever mais uma tese só com agradecimentos!! Merecias um nobel pela paciência em me aturar!! Obrigado pela amizade, pelo apoio e preocupação, por todos os bons momentos que passamos ao longo destes 2 anos que ficarão sempre na memória!

- à Mafalda, que entrou nesta aventura a meio mas que deixou igualmente a sua marca! Obrigado pela amizade incansável, por todo o apoio e força, pela confiança depositada. Obrigado pelas palavras certas no momento certo!

- e por último mas obviamente não menos importante ao PIN, que tão bem me recebeu e integrou! Obrigado por toda a diversão e excelente ambiente de trabalho proporcionados!

Palavras-chave

Drosophila, String/CDC25, Fotorreceptores, homeostasia neuronal, neurodegeneração

Resumo

O ciclo celular e a diferenciação são dois processos altamente coordenados durante o desenvolvimento dos órgãos. Estudos recentes demonstraram que os reguladores do ciclo celular também desempenham funções independentes do ciclo celular em neurónios pós-mitóticos e são essenciais para a manutenção da homeostasia neuronal. As fosfatases CDC25 são conhecidas como ativadores de CDKs e a sua atividade está principalmente associada a tecidos em proliferação. A sua expressão e atividade têm sido descritas em cérebros adultos de mamíferos. Contudo, a sua relevância fisiológica e os seus potenciais substratos nunca foram abordados num contexto não proliferativo. O homólogo de CDC25 em *Drosophila* é codificado por *string (stg)*. Estudos prévios do nosso grupo mostram que *stg* é expresso nos fotorreceptores e nos neurónios da lâmina, que são dois tipos celulares diferenciados que constituem o sistema visual da mosca. Os objetivos deste trabalho são identificar a função de *stg* e os seus potenciais substratos neuronais, utilizando o sistema visual de *Drosophila* como modelo. Para obter informação acerca da função de *stg* utilizámos o sistema GAL4/UAS para reduzir a expressão de *stg* nos fotorreceptores, através de um transgene RNAi. Os defeitos provocados pela perda de função de *stg* foram avaliados no disco imaginal do olho por imunofluorescência, e durante a fase adulta por microscopia eletrónica de varrimento. Esta abordagem genética foi acoplada a uma técnica de proteómica específica, eletroforese diferencial em gel bidimensional (2D-DIGE), para identificar os substratos de Stg nos fotorreceptores. Os nossos resultados mostraram que a redução da expressão de *stg* nos fotorreceptores afetou o padrão de organização da retina, induzindo a perda da manutenção apical do núcleo dos fotorreceptores no epitélio do disco do olho e a desorganização dos omatídios. Também detetámos uma distribuição anormal de proteínas do citoesqueleto e destabilização da estrutura axonal. Consequentemente, a projeção dos axónios para os neurópilos da lâmina e médula do lobo óptico foi perturbada. Após a redução de expressão de *stg,* observamos também que os fotorreceptores acumularam Ciclina B. Apesar do fenótipo olho rugoso observado após redução da expressão de *stg* sugerir neurodegeneração, não detetámos morte neuronal durante a fase larvar, sugerindo que provavelmente ocorre durante a fase de pupa ou do desenvolvimento do adulto. Através da análise por 2D-DIGE identificámos sete proteínas com expressão diferencial que constituem potenciais substratos de Stg nos fotorreceptores. Em conjunto, as nossas observações sugerem que a fosfatase Stg desempenha uma função essencial em neurónios do sistema visual de *Drosophila*, regulando vários componentes e processos celulares para manter a sua homeostasia.

Keywords

Drosophila, String/CDC25, photoreceptors, neuronal homeostasia, neurodegeneration

Abstract

Cell cycle and differentiation are two highly coordinated processes during organ development. Recent studies have demonstrated that core cell cycle regulators also play cell cycle-independent functions in post-mitotic neurons, and are essential for the maintenance of neuronal homeostasis. CDC25 phosphatases are well-established CDK activators and their activity is mainly associated to proliferating tissues. The expression and activity of mammalian CDC25s has been reported in adult brains. However, their physiological relevance and the potential substrates in a non-proliferative context have never been addressed. *string (stg)* encodes the *Drosophila* CDC25 homolog. Previous studies from our group showed that *stg* is expressed in photoreceptors (PRs) and in lamina neurons, which are two differentiated cell types that compose the fly visual system. The aims of this work are to uncover the function of *stg* and to identify its potential neuronal substrates, using the *Drosophila* visual system as a model. To gain insight into the function of *stg* in a non-dividing context we used the GAL4/UAS system to promote downregulation of *stg* in PR-neurons, through the use of an RNAi transgene. The defects caused by *stg* loss-of-function were evaluated in the developing eye imaginal disc by immunofluorescence, and during adult stages by scanning electron microscopy. This genetic approach was combined with a specific proteomic method, two-dimensional difference gel electrophoresis (2D-DIGE), to identify the potential substrates in PR-cells. Our results showed that *stg* downregulation in PRs affects the well-patterned retina organization, inducing the loss of apical maintenance of PR-nuclei on the eye disc, and ommatidia disorganization. We also detected an abnormal accumulation of cytoskeletal proteins and a disruption of the axon structure. As a consequence, the projection of PR-axons into the lamina and medulla neuropils of the optic lobe was impaired. Upon *stg* downregulation, we also detected that PR-cells accumulate Cyclin B. Although the rough eye phenotype observed upon *stg* downregulation suggests neurodegeneration, we did not detect neuronal death during larval stages, suggesting that it likely occurs during pupal stages or during adulthood. By 2D-DIGE, we identified seven proteins which were differentially expressed upon *stg* downregulation, and are potential neuronal substrates of Stg. Altogether, our observations suggest that Stg phosphatase plays an essential role in the *Drosophila* visual system neurons, regulating several cell components and processes in order to ensure their homeostasis.

The results obtained during the development of this project were presented in scientific meetings, in the form of platform and poster presentations, and are part of a manuscript in preparation.

Poster presentations:

- Gonçalves R. and Lopes C. S. (2015). Functional analysis of String/CDC25 phosphatase in post-mitotic neurons. Portuguese *Drosophila* Meeting. Tomar, Portugal.

- Gonçalves R., Monteiro D., Pinho M., Lopes C. S. (2015). The role of String/CDC25 phosphatase in neurodevelopment: an entry point to disease. 24th European *Drosophila* Research Conference. Heidelberg, Germany.

- Gonçalves R. and Lopes C. S. (2014). Functional analysis of String/CDC25 phosphatase in post-mitotic neurons. I3S 4th Annual Meeting. Póvoa de Varzim, Portugal.

Oral communications:

- Gonçalves R. and Lopes C. S. (2015). Functional analysis of String/CDC25 phosphatase in post-mitotic neurons. XXXIX Jornadas Portuguesas de Genética. Braga, Portugal.

TABLE OF CONTENTS

LIST OF ABBREVIATIONS

AD – Alzheimer's disease

APC/C – Anaphase-promoting complex/Cyclosome

ato – atonal

BOSS – Bride of Sevenless

BrdU - bromodeoxyuridine

CadN – N-Cadherin

ci – cubitus interruptus

Caps – Capricious

CD8 – Cluster of differentiation 8

CDC25 – Cell division cycle 25

CDK – Cyclin-dependent kinase

Cy – Cyanine

Cyc B – Cyclin B

DAB – 3, 3'-Diaminobenzidine

dac – dachshund

DER – *Drosophila* epidermal growth factor receptor

Dl – Delta

dpp – decapentaplegic

DTT – Dithiothreitol

EGF – Epidermal growth factor

Elav – Embryonic lethal abnormal vision

eya – eyes absent

ey – eyeless

F-actin – Filamentous actin

FBS – Fetal Bovine Serum

Fmi – Flamingo

FMW – First Mitotic Wave

Fzr – Fizzy-related

Gal4 – Galactose-responsive transcription factor 4

GFP – Green Fluorescent Protein

gcm – glial cells missing

GMR – Glass Multimer Reporter

Gogo – Golden goal

h – hairy

Hh – Hedgehog

hth – homothorax

H_2O_2 – hydrogen peroxide

HMDS – hexamethyldisilazane

HRP – Horseradish peroxidase

IEF – Isoelectric Focusing

Ifs – Intermediate filaments

INM – Interkinetic nuclear migration

KCl – potassium chloride

KH_2PO_4 – monopotassium phosphate

L1 – first instar larvae

L2 – second instar larvae

L3 – third instar larvae

LOF – loss-of-function

LPCs – lamina precursor cells

Lz – Lozenge

MF – morphogenetic furrow

mRNA – messenger RNA

MTs – microtubules

NaCl – sodium chloride

Na_2PO_4 – disodium phosphate

OL – optic lobe

ORC – Origin Recognition Complex

OS – Optic stalk

PATJ – Pals 1-associated tight junction protein

PBS – Phosphate-buffered saline

phyl – phyllopod

PI – isoelectric point

PLK – Polo-like kinase

PMCs – post-mitotic cells

PPase – protein phosphatase

PRs – photoreceptors

pros – prospero

Repo – Reversed polarity

RFP – Red Fluorescent Protein

Rh - rhodopsin

Rho/Phall – Rhodamine/Phalloidin

RNAi – Interference RNA

Ro - Rough

RT-PCR – Real-time Polymerase chain reaction

RT – Room temperature

SDS – Sodium dodecyl sulfate

SEM – Scanning electron microscopy

sens – senseless

Ser – Serine

Sev –Sevenless

Shh – Sonic hedgehog

Sim - Single-minded

SMW – Second Mitotic Wave

Syn - synaptotagmin

so – sine oculis

Spa – Sparkling

Spi – Spitz

stg – string

Thr – Threonine

toy – twin of eyeless

Tyr – Tyrosine

TS – solubilization buffer

UAS – Upstream Activating Sequence

WT – Wild-type

LIST OF FIGURES

LIST OF TABLES

1. Introduction

1.1 *Drosophila melanogaster* as a model system

The fruit fly *Drosophila melanogaster* is a powerful model organism which has been widely used to study a broad range of biological processes, such as genetics, morphogenesis, cell signaling, behavior and aging. There are several reasons that make *Drosophila* an excellent model system: its short life cycle with high reproductive rate; the easiness to handle and to maintain in the lab; its simple food requirement; a very well described anatomy and development; and a wide range of genetic tools available (Jennings, 2011). *Drosophila* has a very short life cycle composed by four stages or instars: egg, larvae, pupa and the adult stage, whose duration varies with temperature. At 25ºC, the life cycle may be completed in approximately ten days (Demerec & Kaufman, 1996). In 22-24 hours, the first instar larvae (L1) emerge from the egg, which then feed on the substrate and undergo several molts until they reach the largest larval form, the third instar larvae (L3). The external structures of the adult organism, such as eyes, head, legs and wings develop during larval stages from primitive cell complexes called imaginal discs. The pupal stage starts approximately 120 hours after the beginning of embryonic development. During this period a series of profound modifications occur (metamorphosis) to complete the formation of the adult organism, including the destruction of certain tissues and organs and the remodeling of others, such the nervous system. At the end of pupal stage, the adult fly emerges from the pupal case and two days later females become sexually active (reviewed in Campos-Ortega & Hartenstein, 1997) (Figure 1).

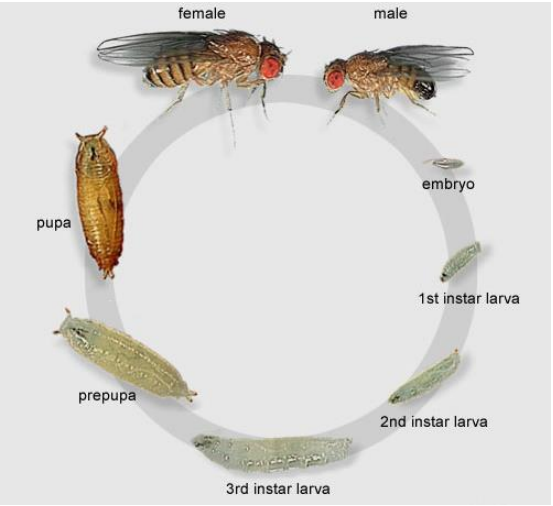

Figure 1. The life cycle of *Drosophila melanogaster*. Females store a considerable amount of sperm in their receptacles for fertilization. The 1st instar larvae (L1) emerge from the egg and undergo two molts to generate the 2nd instar larvae (L2). These, feed on the substrate and grow into the 3rd instar larvae (L3). At the end of larval stages, the L3 larvae undergo pupation and metamorphosis occurs. After metamorphosis, an adult fly emerges from the pupal case. Males become sexually active approximately 12h after the emergence; in the case of females, they only lay eggs two days later (adapted from Jennings, 2011).

1.2 The *Drosophila* visual system

The *Drosophila* visual system has been particularly used to understand several processes, such as cell cycle control, cell fate, pattern formation, and to dissect many signaling pathways (Cagan, 2009; Roignant & Treisman, 2009). The fly visual system is composed by two main structures: externally by the retina and internally by two optic lobes (OL). Each OL is divided into four regions: lamina, medulla, and lobula complex, which includes the lobula and lobula plate (Figure 2). The optic lobes receive and process the visual information sent by specific neuronal cells that compose the retina, called photoreceptors (PRs) (reviewed in Sanes & Zipursky, 2010). The fly compound eye is a highly repetitive and ordered structure which is not essential for fly survival in the lab. Thus, any gain or loss-of-function (LOF) experiment which perturbs the normal eye development will be easily detected on the adult retina, making this an ideal system to generate mosaic animals and to perform genetic screens (reviewed in Silies & Klämbt, 2010).

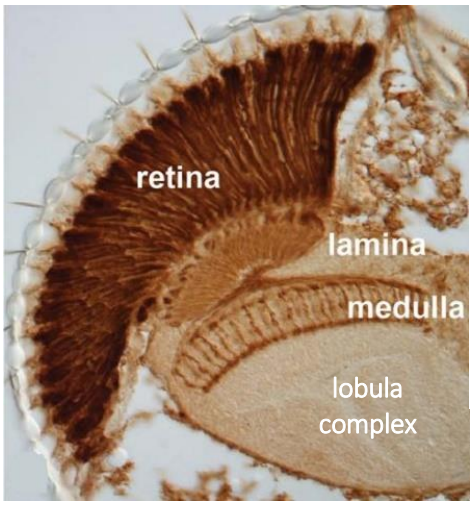

Figure 2. Composition and organization of the fly visual system. Coronal section of an adult fly head stained with anti-β-galactosidase (brown) to show PR-cells. The two main structures that compose the fly visual system can be identified: retina and the OL, composed by the lamina, medula and lobula complex. PR-cells of the retina project their axons into the lamina and medulla neuropils (adapted from Treisman, 2013).

1.2.1 The *Drosophila* compound eye – structure and composition

The *Drosophila* retina is a highly organized structure composed of 750-800 ommatidia or unit eyes organized in a hexagonal array. Each ommatidium is composed by eight PR-neurons, divided into two classes: six outer, R1-R6, which express rhodopsin Rh1, and two inner, R7 and R8, which express Rh5 and Rh6, and Rh3 and Rh4, respectively (Figure 3). These PR-cells project differentially their axons through the optic stalk (OS) into the OL: R1-R6 innervate the lamina, while R8 and R7 project into deeper layers of the OL, innervating the medulla. PR-cells are surrounded by twelve accessory cells, which include four cone cells, which secrete the lens, an array of primary, secondary and tertiary pigment

cells, and mechanosensory bristles (reviewed in Morante *et al.,* 2007; Roignant & Treisman, 2009; Hadjieconomou *et al.*, 2011; Treisman, 2013).

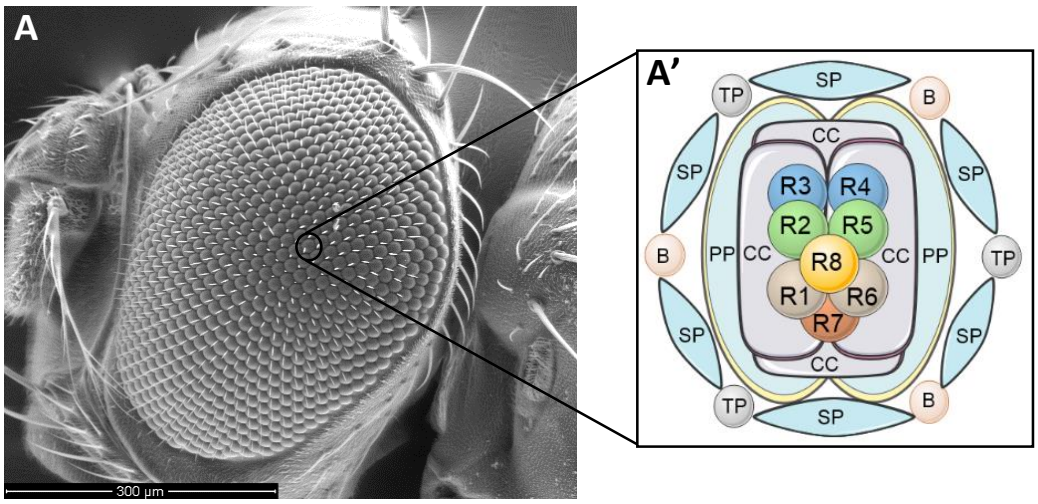

Figure 3. Structure and composition of the *Drosophila* adult eye. Scanning electron micrograph (SEM) of an adult *Drosophila* head (A) showing that the retina is composed by hundreds of ommatidia units (A'), arranged in a highly organized pattern. Each ommatidium (A') is composed by eight PR-neurons (R1-R8) and four cone cells (CC), which are surrounded by a lattice of primary (PP), secondary (SP) and tertiary (TP) pigments cells, and bristles (B) (adapted from Carthew, 2007).

1.2.2 Pattern formation during eye development

The adult fly eye is derived from a bilayered neuroepithelia, the eye imaginal disc, which starts to differentiate during L3 instar of the fly life cycle. The development of the eye imaginal disc into the adult structure is controlled by a conserved retinal determination network composed by several transcription factors, such as *twin of eyeless (toy), eyeless (ey), sine oculis (so), eyes absent (eya)* and *dachshund (dac)* (reviewed in Atkins *et al.*, 2013). During late embryogenesis, *eye* expression is responsible for the specification of eye-progenitor cells in the imaginal disc (Czerny *et al.*, 1999). Ommatidia pattern and differentiation begins during L3 at the posterior margin of the eye disc (Ready *et al.*, 1976). The first sign of differentiation is the appearance of a dorsoventral constriction called morphogenetic furrow (MF), which sweeps the eye disc in a posterior-anterior direction. Cells located anterior to the moving furrow proliferate asynchronously and are maintained in a proliferative and multipotent state due to the expression of *homothorax (hth)*; posterior to the MF cells become progressively differentiated and organized into the nascent ommatidium (Figure 4) (Tomlinson & Ready, 1987; Wolff & Ready, 1991; Bessa *et al.*, 2002).

The critical signal that promotes the initiation and progression of the MF is the morphogen Hedgehog (Hh) (reviewed in Heberlein & Moses, 1995; Roignant & Treisman, 2009). Before MF initiation, cells at the posterior margin of the eye disc express Hh and release this signal to neighboring cells, inducing their differentiation into PRs. As they differentiate, PR-cells express Hh again to promote differentiation of more anterior cells. This gradual spread of *hh* expression ensures the movement of the MF and the differentiation towards the anterior region of the eye disc (Heberlein *et al.*, 1993; Ma *et al.*, 1993; Heberlein & Moses, 1995; Domínguez & Hafen, 1997).

In the eye, Hh signaling leads to the stabilization of full length *cubitus interruptus (ci),* enabling the expression of *dpp (decapentaplegic)* in cells within the MF (Fu & Baker, 2003; Pappu, 2003). Dpp represses *hth* expression enabling cell cycle exit and hence the differentiation of progenitor cells (Bessa *et al.*, 2002). Simultaneously to *hth* repression, the *Drosophila cdc25* homologue *string (stg)* is upregulated immediately anterior to the MF driving retinal progenitors through the first mitotic wave (FMW) into G1 arrest (Thomas, 1994; Lopes & Casares, 2010). The expression of *so, ey* and *eya* in retinal progenitor cells promotes the expression of *atonal (ato)* (Zhang *et al.*, 2006). Dpp also induces the upregulation of *hairy (h)* in cells anterior to the MF (Greenwood & Struhl, 1999), and the expression of the ligand for Notch receptor Delta (Dl) in cells within the MF (Fu & Baker, 2003; Baonza & Freeman, 2005). Hairy acts as a repressor of *ato,* preventing a premature differentiation. Through Notch-mediated lateral inhibition, *ato* expression becomes restricted to a single R8 precursor cell, being the first PR to be specified. Then, the R8 founder PR recruits sequentially the other PR-cells through inductive signals: first R2/R5 and then R3/R4, generating a five-cell precluster. This precluster is maintained in G1 arrest while the surrounding undifferentiated cells undergo a final cell division, at the second mitotic wave (SMW), to generate the remaining cells of the ommatidium. These remaining cells are also recruited orderly: R1/R6, R7 and four cone cells. Already during pupal stage, an array of pigment cells (primary, secondary and tertiary) and bristles are added completing the ommatidium (Figure 4) (Tomlinson & Ready, 1987; Wolff & Ready, 1991; Freeman, 1996).

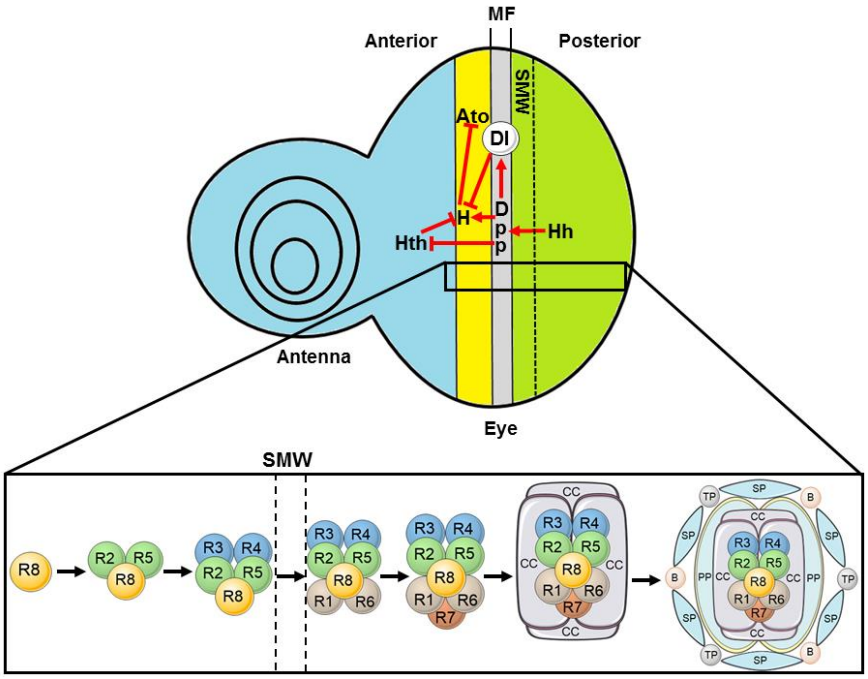

Figure 4. Schematic representation of ommatidia assembly in the developing eye. The adult eye is derived from the eye-antenna imaginal disc. The differentiation of the eye imaginal disc starts during L3 and the MF is the first sign of this process. Hh is a determinant signal for the initiation and progression of the MF. Hh is expressed in cells posterior to the MF and spreads onto more anterior cells, inducing their differentiation into PRs. The repression of *hth* in retinal progenitors mediated by Dpp induces cell cycle exit and differentiation. Notch-mediated lateral inhibition is essential to restrict *ato* expression in a single R8 precursor cell, being the first PR to be specified. The remaining cells are recruited and added into the developing ommatidia in an orderly and sequentially manner: R2/R5, R3/R4, R1/R6, R7, and finally accessory cells (cone and pigment). All cell types except the five-cell precluster (R8, R2/R5, R3/R4) are generated during the SMW (adapted from Clandinin & Zipursky, 2002; Roignant & Treisman, 2009).

1.2.3 Cell specification in the developing eye

Cell fate determination during eye development occurs through a combination of specific signals released by neighboring cells and cell-cell interactions. In 1996, Freeman described a cell fate mechanism taking into account the dynamic activity of the *Drosophila* epidermal growth factor receptor (DER). After R8 specification, which occurs under the control of *ato*, R8 expresses two proteins that control DER activity: Spitz (Spi) and Argos. Spi accumulates in precursor cells recruited by R8, activating DER signaling and consequently inducing their differentiation into R2 and R5; simultaneously, Argos spreads further and acts as a repressor of DER activity in more distant cells by inhibiting their neuronal specification. Then, R2 and R5 also express Spi and Argos, inducing the specification of R3 and R4 in a similar manner. The other cell types follow the same mechanism of specification with the exception of R7 (Freeman, 1996). The R7 specification

depends of the receptor tyrosine kinase Sevenless (Sev) and the ligand Bride of Sevenless (BOSS). *sev* is exclusively required for R7 specification (Tomlinson & Struhl, 2001), while BOSS is expressed by R8 (Simon, 1994). The binding of BOSS into Sev of pre-R7-cells activates a signal cascade that leads to R7 specification (Simon, 1994; Tomlinson & Struhl, 2001). Besides the importance of EGF signaling, retinal progenitors also express other proteins which also contribute for their cell fate decisions, such as Senseless (Sens) for R8, and Prospero for the R7 equivalence group (R1, R6, R7 and cone cells) (Crew *et al.*, 1997; Shi & Noll, 2009). All these genes are presented below in Table 1.

Table 1: Genes involved in cell specification during retina development

Cell type	Key elements for cell fate	References
R8	*atonal (ato)*	Dokucu *et al.*, 1996; Domínguez, 1999; Lim & Choi, 2004
	bride of sevenless (boss)	Hart *et al.*, 1990; Freeman *et al.*, 1992
	senseless (sens)	Frankfort & Mardon, 2002
R2/R5	*rough (ro)*	Kimmel *et al.*, 1990
	rhomboid	Freeman *et al.*, 1992
R3/R4	*rough (ro)*	Kimmel *et al.*, 1990
	spalt	Domingos *et al.*, 2004
R1/R6	*seven-up (svp)*	Kramer *et al.*, 1995
	bar	Higashijima *et al.*, 1992
	lozenge (lz)	Crew *et al.*, 1997
	phyllopod (phyl)	Chang *et al.*, 1995; Dickson *et al.*, 1995
	prospero (pros)	Charlton-Perkins *et al.*, 2011
R7	*lozenge (lz)*	Crew *et al.*, 1997
	phyllopod (phyl)	Freeman *et al.*, 1992; Chang *et al.*, 1995; Dickson *et al.*, 1995
	prospero (pros)	Charlton-Perkins *et al.*, 2011
	sevenless (sev)	Tomlinson & Struhl, 2001
Cone cells	*lozenge (lz)*	Crew *et al.*, 1997
	prospero (pros)	Charlton-Perkins *et al.*, 2011
	sparkling (spa)	Fu & Noll, 1997
Pigment cells	*lozenge (lz)*	Crew *et al.*, 1997
	sparkling (spa)	Fu & Noll, 1997

1.2.4 Interkinetic nuclear migration during photoreceptor development

Nuclear positioning plays an important role in tissue architecture. During eye development, mitosis of undifferentiated cells occurs on the basal domain of the eye imaginal disc. For the differentiation of PRs, retinal precursors exit the cell cycle and nuclei migrate into the final position, the apical surface (Fan & Ready 1997). This nucleus movement was described by Sauer in 1935 as interkinetic nuclear migration (INM) and it contributes to the apical arrangement of post-mitotic cells (PMCs), creating space on the basal domain for other mitotic cells (Murciano *et al.*, 2002).

Evidences suggest that microtubules (MTs) and associated motor proteins are involved in INM (reviewed in Taverna & Huttner, 2010). Motor proteins perform long distance movements along the axons transporting several cargos, such as nuclei, vesicles and organelles (Chevalier-Larsen & Holzbaur, 2006). From basal-to-apical, nuclei are transported by the minus-end-directed MT-associated dynein; from apical-to-basal, the movement of nuclei is performed by the plus-end-directed kinesin motor system (Baye & Link, 2008). Whited *et al.* (2004) suggested that the position of PR-nuclei within the *Drosophila* eye imaginal disc depends on the balance of the opposing activities of dynein/dynactin and kinesin (Whited *et al.*, 2004). They demonstrated that mutations in the dynactin subunit Glued lead to a strong displacement of the PR-nuclei from the apical surface, into the OS and the brain. Also using *Drosophila* as a model, Martin *et al.* (1999) showed that mutations in both dynein/dynactin and kinesin result in an inhibition of axonal transport (Martin *et al.*, 1999). However, in the zebrafish retinal neuroepithelium, actomyosin contractility has been described as the main driver of INM (Norden *et al.*, 2009; Schenk *et al.*, 2009). In the actomyosin-based transport, the nuclei are moved along the actin filaments in a myosin II-dependent manner (Norden *et al.*, 2009). In this process, myosin II contracts the actin cytoskeleton generating forces for the movement of nuclei in a particular direction. Inhibiting myosin II, the nuclei movement is substantially reduced (Schenk *et al.,* 2009).

INM is closely linked to the differentiation of PR-cells (Whited *et al.*, 2004). The nuclei migration along the apical/basal axis may facilitate different cellular responses to intrinsic signals resulting in the activation of different surface receptors, which in turn promote different effects on gene regulation and ultimately leads to different cell fate decisions (Murciano *et al.*, 2002; Baye & Link, 2008).

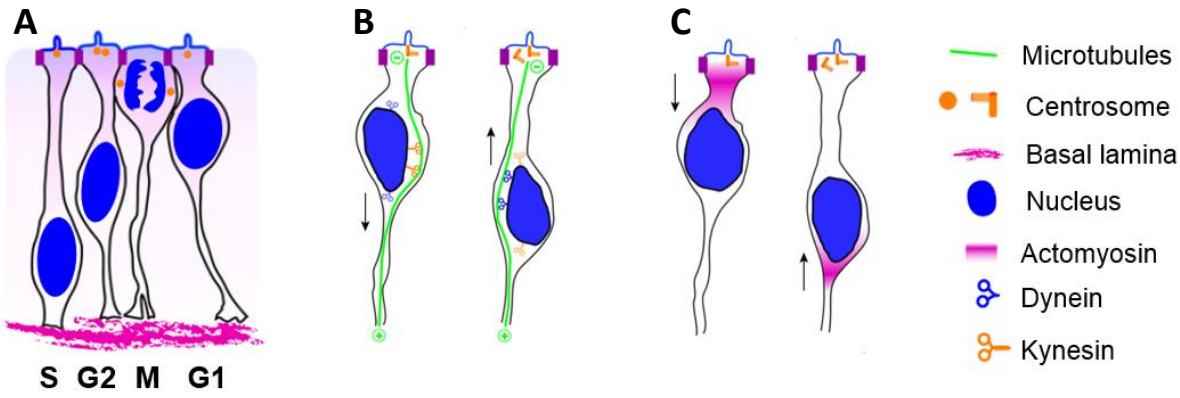

Figure 5. Interkinetic nuclear migration in neuroepithelial tissues. A) Nuclei migrate along the apical/basal axis, displaying a particular localization on the epithelium during each step of the cell cycle. Post-mitotic nuclei migrate into the apical surface, generating space basally for new mitotic cells. B) MT-associated motor proteins, such as dynein and kinesin, are involved in nuclei migration along the apical-basal axis. Dynein transport nuclei basal-to-apical, while kinesin performs the opposite movement, placing nuclei away from the apical domain. C) Actomyosin is also involved in INM, where nuclei are transported through myosin II-generating forces (adapted from Taverna & Huttner, 2010).

1.2.5 Photoreceptors generate a retinotopic map with the optic ganglia

1.2.5.1 Photoreceptors are essential mediators of lamina formation and differentiation

As PR-cells differentiate, they extend axons through the OS establishing connections with specific regions of the optic ganglia: lamina and medulla (Hadjieconomou *et al.*, 2011; Morante & Desplan, 2013). Besides the importance for the proper neuronal transmission into the brain, the establishment of this projection pattern is also essential for the generation and differentiation of some cell types that constitute the optic ganglia, such as lamina neurons. This process involves two signals: Hh and Spi. Hh is produced by PR-cells, transported along their axons and released in lamina precursor cells (LPCs) at the OL. In LPCs, Hh activates Ci triggering the final cell division to generate lamina neurons (Figure 6A). Hh also induces the expression the transcription factor Single-minded (Sim), which is responsible for the organization of lamina neurons in columns, and the EGF receptor. Thus, LPCs are competent to respond to a second signal released by other PR-cells, Spi, and finally to differentiate into five lamina neurons L1-L5. Differentiated lamina neurons express the differentiation marker Dac (reviewed in Hadjieconomou *et al.*, 2011).

1.2.5.2 Axon guidance and projection pattern into the brain

The PR projection pattern is gradually generated in the same order as PR differentiation occurs. As R1/R6 differentiate, they progressively project only one bundle into the lamina. During early pupal stage, R1/R6 growth cones project laterally establishing synaptic connections with lamina neurons (Figure 6 A). Unlike R1/R6, lamina neurons extend into the medulla (Figure 6 B). Some studies have reported that the non-classical cadherin Flamingo (Fmi) guides R1/R6 axons into the lamina in a non-autonomous manner through repulsive and attractive interactions among neighbor growth cones. The classical N-cadherin (CadN) seems to be important for lateral projection of R1/R6 (reviewed in Clandinin & Zipursky, 2002; Hadjieconomou *et al.*, 2011).

Glial cells also play an important role in axon guidance. Glial cells are derived from glial progenitors localized in the OL (Choi & Benzer, 1994). Neurogenesis and gliogenesis are closely linked: when neurogenesis in the eye imaginal disc is initiated, Hh expressed by PR-cells triggers glial migration onto the imaginal disc. Thus, as the MF sweeps across the eye disc, the carpet and perineurial glial cells start to extend into the imaginal disc. When the first neuron-glia contact occurs, the perineurial glia differentiates into wrapping glia, which wraps and guides the developing PR-axon into their final target (Choi & Benzer, 1994). Glial cells act as an intermediate target of R1/R6 axons (Poeck *et al.*, 2001). Before differentiation of LPCs, R1/R6 project a single axon into two layers of lamina glia, which provide a still unknown signal to stop their extension (Poeck *et al.*, 2001). In mutants where glia do not migrate (*e.g*. *glial cells missing (gcm), gcm2, nonstop)* into their target region, PR-axons fail to stop in the lamina and continue to project into the medulla (Poeck *et al.*, 2001; Chotard *et al.*, 2005).

R7 and R8 project initially their axons into the medulla surface, close to each other (Fischbach & Dittrich, 1989; Morante *et al.*, 2007), and during pupal stage they project and branch into different medulla layers: R8 extend axons into the M3 layer, while R7 terminates in the M6. Evidences showed that R8 targeting depends on three cell surface proteins which are dynamically expressed: Fmi, the transmembrane protein Golden goal (Gogo) and the leucine-rich repeat Capricious (Caps) (Shinza-Kameda *et al.*, 2006; Tomasi *et al.*, 2008). R7 targeting depends only on CadN (Lee *et al.*, 2001). In the absence of some of these proteins, PR-axons do not project properly into their target region (Lee *et al.*, 2001; Shinza-Kameda *et al.*, 2006; Tomasi *et al.*, 2008).

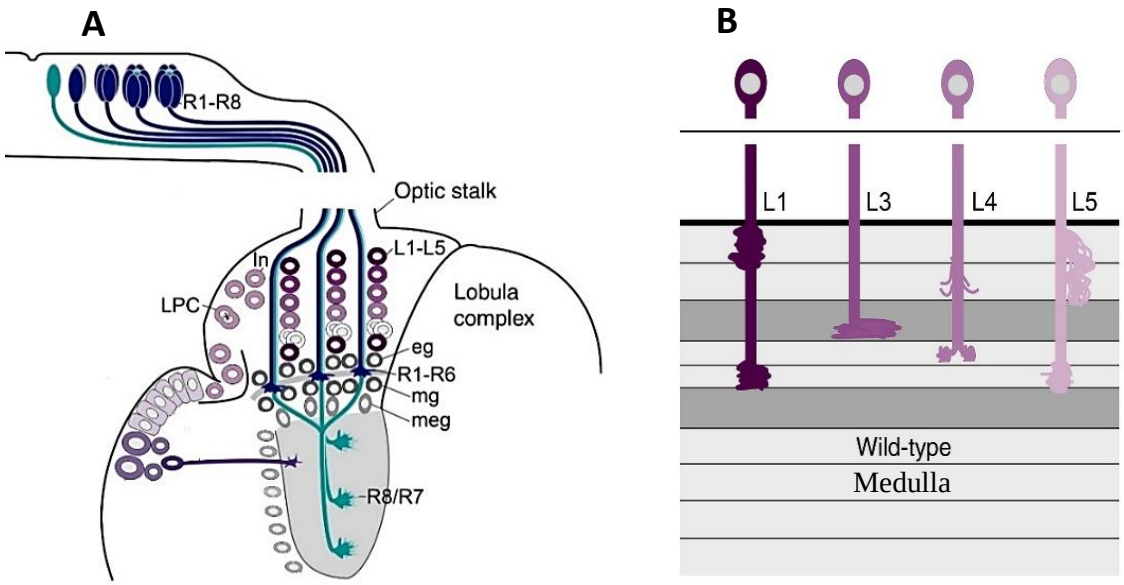

Figure 6. PR projection pattern into the optic ganglia. A) As differentiation occurs, PR-cells progressively extend axons into specific regions of the optic ganglia: R1/R6 terminate in lamina neurons (ln), while R8 and R7 terminate in M3 and M6 layers of the medulla, respectively. PR-cells are also essential for differentiation of lamina neurons. PRs express Hh, which is transported and released in lamina precursor cells (LPCs), inducing their final cell division and ultimately their differentiation into L1-L5 lamina neurons. Glial cells plays a critical role in R1/R6 guidance. In the optic ganglia, glia migrates close to the LPCs and send a still unknown signal to stop axon elongation. After LPC differentiation, R1/R6 establish synaptic contacts with L1-L5. B) Lamina neurons also extend axons into specific layers of the medulla. **eg**, epithelial glia; **mg**, marginal glia; **meg**, medulla glia (adapted from Clandinin & Zipursky, 2002).

1.2.6 The role of cytoskeleton in axonal transport and growth

1.2.6.1 Neuronal cytoskeleton and axonal transport

Cytoskeleton is a crucial cell component that provides structural support and shape during development. In neurons, cytoskeleton comprises three main components: MTs, actin and intermediate filaments (IFs) (Hirokawa & Takemura, 2004). MTs are highly dynamic αβ-tubulin dimers which polymerize from the centrosome, the MT-organizing center (Leavens, 2007). They are present along the axon shaft and in the neuron tips, called growth cones. At the growth cones, MTs orientation predicts the direction of outgrowth (Sabry *et al.*, 1991).

Along the axon shaft, together with MT-associated motor proteins such dynein and kinesin, MTs are involved in intracellular transport of several cargos (*e.g.* mitochondria, vesicles, RNAs) (Welte, 2004; Chevalier-Larsen & Holzbaur, 2006). In this process, dynein performs the retrograde movement, transporting cargos toward the nucleus, while kinesin

is responsible for the anterograde movement, away from the cell body (Hirokawa & Takemura, 2004) (Figure 7). In mutants for the *Drosophila* kinesin-1 have been observed an accumulation of several cargos, such as mitochondria, vesicles and synaptic membrane proteins, resulting in swellings along the axons. As a consequence of axon swellings, both retrograde and anterograde transports are disrupted (Hurd & Saxton, 1996). Mutations in subunits of the *Drosophila* dynactin (*e.g.* Glued) are also known to inhibit the axonal transport (Harte & Kankel, 1983).

The proper transport of mitochondria is also important to ensure the energy required in specific regions of cell. Mitochondria are produced in the cell body, transported to the growth cones where energy is required for axon growth, and then return to the cell body for degradation (Morris & Hollenbeck, 1993). Mitochondrial dysfunctions has been associated to excitotoxicity and oxidative stress, which appears to be involved with some neurodegenerative disorders (Manfredi & Xu, 2005).

1.2.6.2 Cytoskeleton remodeling during axon outgrowth

Axonal outgrowth is characterized by extension or retraction of membrane protrusions called filopodia and lamellipodia (Dent & Gertler, 2003). During this process, both actin and MT cytoskeleton undergo a continuous remodeling to provide force and structural support for axon extension. This remodeling requires a highly coordination of actin and MT dynamics, where actin and MT regulators play an important role controlling the polymerization/depolymerization and stability of filaments (Dent & Gertler, 2003). Several evidences reported the involvement of many signals in neuronal outgrowth and guidance (*e.g*. Sonic hedgehog (Shh)) (Avilés *et al.*, 2013). In response to a positive signal, MTs in the cell body become stabilized and are transported into the neuronal cortex. Actin nucleators and barbed-end binding proteins are also activated to promote actin polymerization, and consequently filopodia and lamellipodia are produced. To support the growth, actin severing proteins are also activated to create new actin barbed-ends. F-actin bundles are crucial for MT guidance and stabilization into the protrusions. In specific regions of lamellipodia, F-actin is lost to allow MT elongation but in other positions generates arcs (actin-arcs) to control this elongation (Figure 7). These findings suggest that a tight regulation and coordination of neuronal actin and MT cytoskeleton is crucial for axon outgrowth toward their targets (Dent *et al.*, 2011; Prokop *et al.*, 2013).

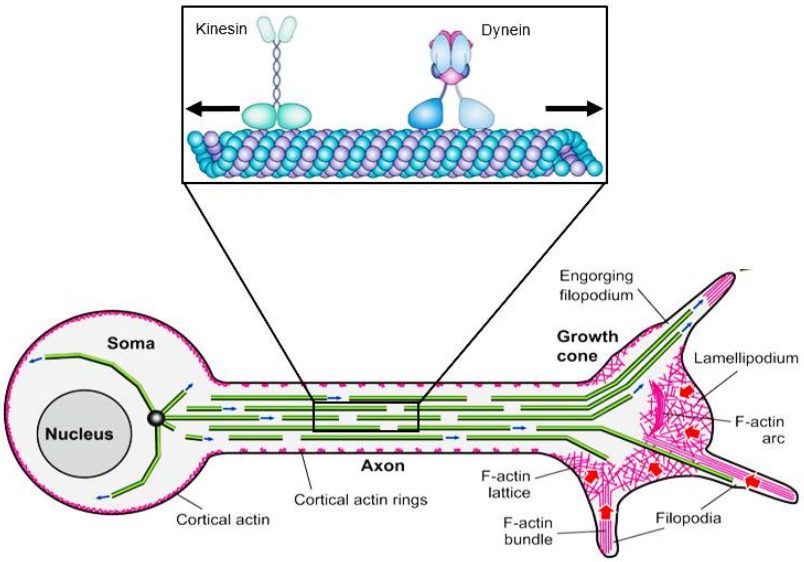

Figure 7. Schematic representation of neuronal cytoskeleton dynamics. MTs polymerize in the centrosome and then extend along the axon shaft towards the growth cone. MT bundles along the axon shaft are essential for intracellular transport mediated by dynein and kinesin. The movement of MTs into the neuronal cortex implies a rearrangement of actin cytoskeleton. F-actin bundles are generated to guide MT extension in the direction of growth. Regions devoid of actin in lamellipodia also contribute to MT elongation. F-actin arcs are also generated to control MT elongation (adapted from Prokop *et al.*, 2013).

1.3 The role of cell cycle regulators in a post-mitotic context

Cell cycle and differentiation are two highly regulated and coordinated processes crucial during development. Cell cycle progression is tightly regulated by a core of cell cycle regulators, which include cyclin-dependent kinase (CDK) inhibitors (p27, p57), transcription factors (Retinoblastoma and E2F3), Anaphase-promoting complex/Cyclosome (APC/C), and some kinases (Polo-like kinase 2 (PLK2)) (reviewed in Herrup & Yang, 2007; Frank & Tsai, 2013). However, recent studies have reported that these regulators also exert many cell cycle-independent functions in post-mitotic neurons (K. L. Ferguson *et al.*, 2005; Nguyen *et al.*, 2007; Kim *et al.*, 2009). Their roles in a non-proliferative context are related with neuronal migration, axonal elongation, axon pruning, dendrite morphogenesis and synaptic plasticity, which are essential for the maintenance of neuronal homeostasis (reviewed in Frank & Tsai, 2009). Some of these functions have also been described in *Drosophila*. Studies using *Drosophila* mushroom body neurons identified two cohesion subunits, SMC1 and SA, whose LOF experiments revealed its importance for axon pruning (Schuldiner *et al.*, 2009). Origin recognition complex (ORC) proteins and APC/C also appear to play important functions in the *Drosophila* nervous system. Pinto *et al.* (1999) reported that the ORC subunit *latheo* is important for the proper brain architecture, which

fails to occur in *latheo* mutants (Pinto *et al.*, 1999). Silies and Klambt (2010) showed that APC/$C^{Fzr/Cdh1}$ controls glia migration regulating the subcellular localization of adhesiveness molecules, such as Fas2, between neurons and glial cells (Silies & Klämbt, 2010).

1.3.1 Cell division cycle 25 (CDC25) phosphatase – a key regulator of cell cycle progression

CDC25 is a family of Ser/Thr phosphatases that dephosphorylate inhibitory Ser, Thr and Tyr residues on CDKs (Karlsson-Rosenthal & Millar, 2006; Boutros *et al.*, 2007). Specifically, CDC25 dephosphorylates CDK1 of the CDK1/Cyclin B complex, triggering mitosis (Gabrielli *et al.*, 1996; Lindqvist *et al.*, 2005). The first *cdc25* gene was identified in fission yeast as a temperature sensitive mitotic inducer (Russell & Nurse, 1986). In mammals, three related genes were described: *cdc25a*, *cdc25b* and *cdc25c*, which functionally complement the $cdc25^{ts}$ strain (Galaktionov & Beach, 1991). CDC25A localizes predominantly in the nucleus and acts as a rate-limiting controller of the G1/S transition (Busino *et al.*, 2004). CDC25B is the critical initiator of mitosis. It activates CDK1/Cyclin B at the centrosome, which is essential for spindle assembly and MT reorganization (Gavet & Pines, 2010). CDK1/Cyclin B is then translocated into the nucleus, where it is full activated by CDC25C (Lammer *et al.*, 1998; Lindqvist *et al.*, 2005). Finally, a mutual phosphorylation among CDC25s and CDK1/Cyclin B in the nucleus generates an auto-amplification loop that is crucial to promote mitotic entry (Hoffmann *et al.,* 1993). Although each isoform controls differentially G1/S, G2/M and mitosis, Ferguson *et al.* (2005) reported a normal development of double knockout mice $cdc25b^{-/-}$; $cdc25c^{-/-}$, suggesting that CDC25A was able to perform all CDC25 functions (A. M. Ferguson *et al.*, 2005).

1.3.2 String phosphatase – the *Drosophila* mitotic inducer

Drosophila encodes two CDC25 homologs, *stg* and *twine*. Stg is a mitotic inducer and regulates this process by dephosphorylating CDK1 of the CDK1/Cyclin B complex. LOF mutations in *stg* induce G2 arrest in both embryos and imaginal discs, while its ectopic expression leads to a rapid mitotic entry (reviewed in Lehman *et al.*, 1999).

Alphey *et al.* (1992) described that in WT L3 eye imaginal discs, *stg* expression is upregulated in retinal precursor cells immediately adjacent and anterior to the MF (Figure 8 A, arrows) (Alphey *et al.*, 1992). Unpublished results from our group showed that *stg* is also expressed in differentiated cells, posterior to the MF (Figure 8 A, asterisks) and in lamina neurons of the OL (Figure 8 B). In the *Drosophila* eye, *stg* is essential for the synchronization

of retinal precursor cells, driving them into mitosis and subsequent G1 arrest (reviewed in Lehman *et al.*, 1999; Mozer & Easwarachandran, 1999). Mozer *et al.* (1999) showed that loss of *stg* in retinal precursors leads to a G2 arrest and consequently pattern defects. They analyzed *ato* expression in these mutants and no modification was detected, meaning that *stg* is not essential for the onset of pattern formation (Mozer & Easwarachandran, 1999). Despite this, in a non-proliferative context, the physiological role and the potential substrates of *stg* remains elusive.

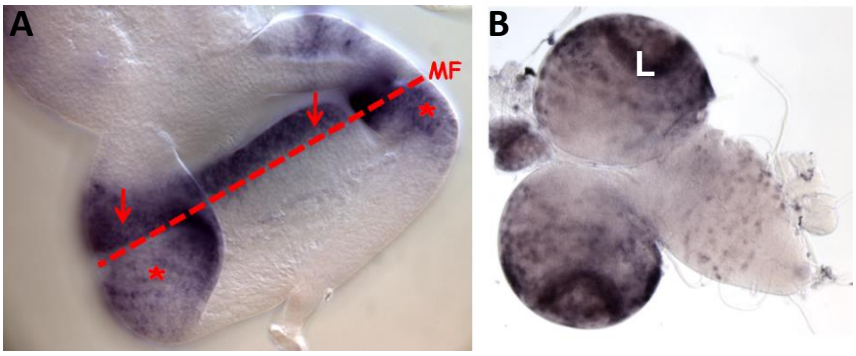

Figure 8. *stg* expression in the developing eye. *in situ* hybridization of *stg* mRNA in L3 eye imaginal disc (A) and in the larval brain (B) are shown. In the eye imaginal disc, a burst of *stg* expression was observed in retinal precursor cells anterior to the MF (arrows); *stg* mRNA was also detected in post-mitotic cells localized posteriorly (asterisks). In the brain (B), *stg* mRNA is highly expressed in lamina neurons (L) (Lopes *et al.*, unpublished).

1.4 Aims of the work

The main goals of this work are to uncover the function of Stg and its substrates in post-mitotic neurons, using the *Drosophila* visual system as a model. This question is of key importance since the mammalian CDC25s are expressed in adult healthy brains and their expression levels and activities are increased in some neurodegenerative disorders, such as Alzheimer's disease (AD), comparing to non-diseased human samples (Chang *et al.*, 2012). To gain insight into the function of *stg*, we used the Gal4/UAS system to promote downregulation of *stg* in PR-cells, and the phenotype was characterized in the developing eye and in adult stages. This genetic approach was combined with a specific proteomic approach, two-dimensional difference gel electrophoresis (2D-DIGE), to identify the substrates of Stg in this post-mitotic context.

2. Material and methods

2.1 The GAL4/UAS system

The Gal4/UAS system is a powerful genetic tool used in *Drosophila* to target gene expression in a tissue-specific and temporal manner (Brand & Perrimon, 1993; Duffy, 2002). This bipartite approach is based on two different transgenic fly lines, the driver line and the responder line: the driver line carries the gene for the yeast transcription factor GAL4, which is under the control of a specific promoter; the responder strain carries the gene of interest fused downstream to a DNA-binding motif of GAL4 called Upstream Activating Sequence (UAS). In the absence of GAL4, the target gene is not transcribed. The GAL4 activity varies with the temperature: at 16ºC its activity is minimal, while at 29ºC its activity is maximal without affecting the fertility and viability of the flies (Duffy, 2002). After crossing these two transgenic lines, in the progeny, GAL4 binds to the UAS sequence activating the expression of the target gene, which is restricted to GAL4-expressing tissues (Brand & Perrimon, 1993; Brand & Dormand, 1995) (Figure 9).

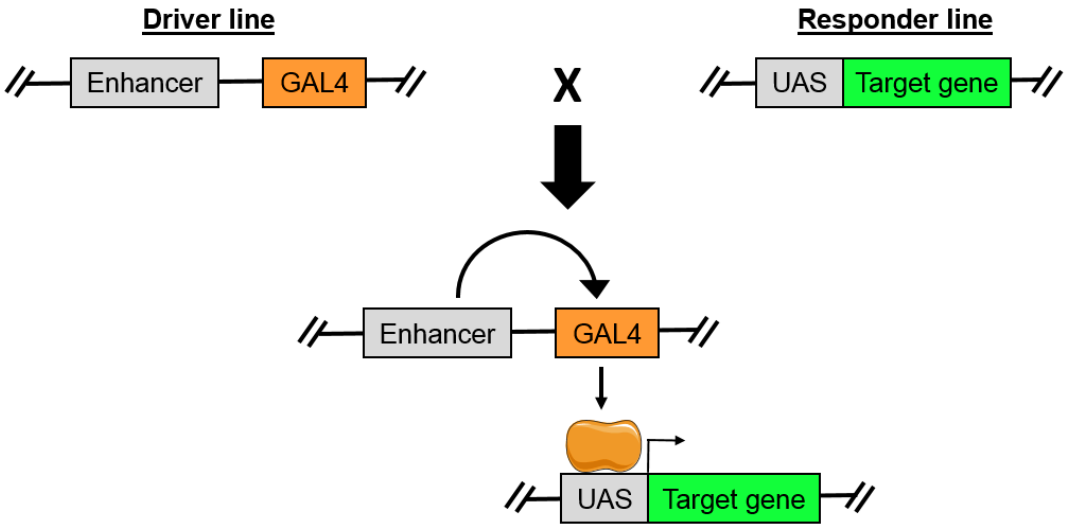

Figure 9. The GAL4/UAS system. Transgenic fly lines carrying the yeast transcription factor GAL4, under the control of a specific promoter, are crossed with a different transgenic line that contains the gene of interest under the control of UAS sequence. In the resulting progeny, the target gene is expressed in a specific pattern that reflects the GAL4 expression pattern (adapted from Duffy, 2002).

2.1.1 Fly handling and genetics

All fly stocks used in this work were propagated on standard food (composition in Table 2) and maintained at 25ºC and 29ºC; crosses were performed in the same conditions through standard genetic techniques (Table 3).

Table 2. Composition of the fly food

Food for stock maintenance				**Food for crosses**		
Components	**V_f = 7.5 L**	**T (ºC)**		**Components**	**V_f = 7.5 L**	**T (ºC)**
H_2O	3.25 L	70		Sugar	750 g	110
Agar	62.5 g	80-85		Yeast	750 g	
Corn flour	500 g	99		Agar	56.3 g	
Soya flour	62.5 g			Cornmeal	375 g	
Yeast	112.5 g			Propionic acid	37.5 mL	65
Malte extract	125 g			Nipagin	188 mL	
Molasses	210 mL					
Nipagin + EtOH	6.25 g	51				
Phosphoric acid	2.5 mL					
Propionic acid	45.5 mL					

Table 3. Fly stocks and genetics

	Genotype	Utility	T (ºC)	References
GAL4 lines	GMR-Gal4 ; ;	*stg* downregulation in all cell types posterior to the MF	25	Freeman, 1996
	P{w[+mW.hs]=GawB}elav[C155], P{w[+mC]=UAS-mCD8::GFP.L}Ptp4E[LL4], P{ry[+t7.2]=hsFLP}1, w[*] ; ;	*stg* downregulation in PR-cells	29	Bloomington Drosophila Stock Center
	P{w[+mW.hs]=GawB}elav[C155] ; ;	Analysis of actin cytoskeleton	25	
	Y[1] w[*] P{w[+mC]=UAS-mCD8::GFP.L}Ptp4E[LL4]P{w[+mW.hs]=GawB}lz[gal4] ; ;	*stg* downregulation in cone cells	25	
	P{w[+mC]=spa-GAL4.J}1, w[*] ; ;			
	GMR:P53, y^1 w^{18}/FM7C	Positive control for Caspase 3	29	
UAS lines	y[1] sc[*] v[1] ; ; P{y[+t7.7] v[+t1.8]=TRiP.HMS00146}attP2	RNAi transgene for *stg*	25/29	
	w; UAS-Lifeact/CyO; mKRS/TM6B	Analysis of actin cytoskeleton	25	
	w[1118] ; ; P{w[+mC]=UAS-stg.N}4	*stg* overexpression in PR-cells	25	
	yw^{122}; ; UAS-GFP/CyO	Reporter for Gal4 expressing cells	25	
	w[1118] ; ; PBac{y[+mDint2] w[+mC]=UAS-CD4-tdGFP}VK00033			
Other lines	*w*; ; *stg*-Trap/TM3	Readout of Stg expression	25	
	w^{1118}; ;	Wild-type control flies	25/29	

2.2 Immunohistochemistry

Eye-antenna imaginal discs were dissected and fixed according to standard protocols. L3 eye discs were dissected in 1X PBS (700 mM NaCl, 10 mM KCl, 50 mM Na_2HPO_4, 9 mM KH_2PO_4; pH 7.4), fixed in 3.7% formaldehyde (Sigma-Aldrich) in 1X PBS for 20 min, and then washed three times with 1X PBS + 0.3% Triton X-100 (PBT 0.3%) for 15 min, all at room temperature (RT). Samples were incubated with primary antibodies in PBT 0.3% overnight at 4ºC, followed by three washes with PBT 0.3% for 15 min. Then, samples were incubated with secondary antibodies in 1X PBS + 0.1% Triton X-100 (PBT 0.1%) for 2h at RT and washed three times with PBT 0.1%. After washes, the solution was replaced by 50% glycerol in 1X PBS and kept at 4ºC. Eye discs were mounted in 50% glycerol (or 80%) in 1X PBS. The primary antibodies used were: rat anti-Elav at 1:400, mouse anti-Futsch at 1:100, mouse anti-Cut at 1:100, mouse anti-Lamin (DM1 and DM2) at 1:100, mouse anti-Prospero at 1:50, mouse anti-Rough at 1:30, mouse anti-Repo at 1:10, mouse anti-Cyclin B at 1:10 (Developmental Studies Hybridoma Bank); rabbit anti-GFP at 1:1000 (Invitrogen), and rabbit anti-Caspase 3 at 1:250 (Cell Signaling Technology). For Caspase-3 assay, the primary antibody was incubated with PBT 0.3% and FBS 0.3%. The secondary antibodies used were Alexa fluor® 488, 568 and 647 (Molecular Probes). Image acquisition of immunostained samples was achieved using the Laser Scanning Confocal Microscope Leica SP2 AOBS SE (Leica Microsystems).

Immunoperoxidase staining was also performed. L3 eye-antenna imaginal discs were dissected, fixed and treated as described above, with the exception that mouse anti-HRP (Santa Cruz Antibodies) (1:400) was used as a secondary antibody in PBT 0.1% for 2h at RT, followed by three washes with PBT 0.1% for 15 min. After washes, samples were incubated with 1 mL of Vectastain solution (VECTASTAIN Elite ABC Kit, VECTOR Laboratories) for 30 min, followed by three washes with PBT 0.1% for 15min. Eye discs were incubated with 3µl of DAB in 300 µl of PBT 0.1% for 5 min and then 3µl of H_2O_2 were added. The staining reaction was stopped by adding PBT 0.1%. Finally, samples were washed three times with PBT 0.1%, the solution was replaced by 50% glycerol in 1X PBS and samples were kept at 4ºC. Eye imaginal discs were mounted as described above. Image acquisition of immuno-labeled tissues was achieved using the Olympus Optical Microscope (Olympus DP 25 Camera; software Cell B). Imaging treatment was performed by Adobe Photoshop® and ImageJ®.

2.3 Two-dimensional difference gel electrophoresis (2D-DIGE)

2D-DIGE is a highly performance and accurate proteomic approach used to identify proteins differentially expressed among several protein samples. The high sensibility of 2D-DIGE allows to detect subtle changes in protein expression and low abundant proteins. The use of a mixed-sample as an internal standard reduces the inter-gel variability. In this method, each sample is labelled covalently with cyanine dies (Cy2, Cy3 or Cy5), which have specific fluorescent properties and have no effects on protein electrophoretic mobility. Then, these samples are mixed and separated on a single gel on basis of molecular weight and isoelectric point (PI). Using and advanced scanner, each 2D gel pattern of the individual protein pools is resolved by specific fluorescent excitation for either dyes (488nm for Cy2, 532nm for Cy3 and 633nm for Cy5). Finally, differentially expressed and/or modified peptides are picked and analyzed by mass spectrometry, which together with bioinformatics identify and characterize each protein (Figure 10) (reviewed in O'Farrell, 1975; Debasish *et al.*, 2013).

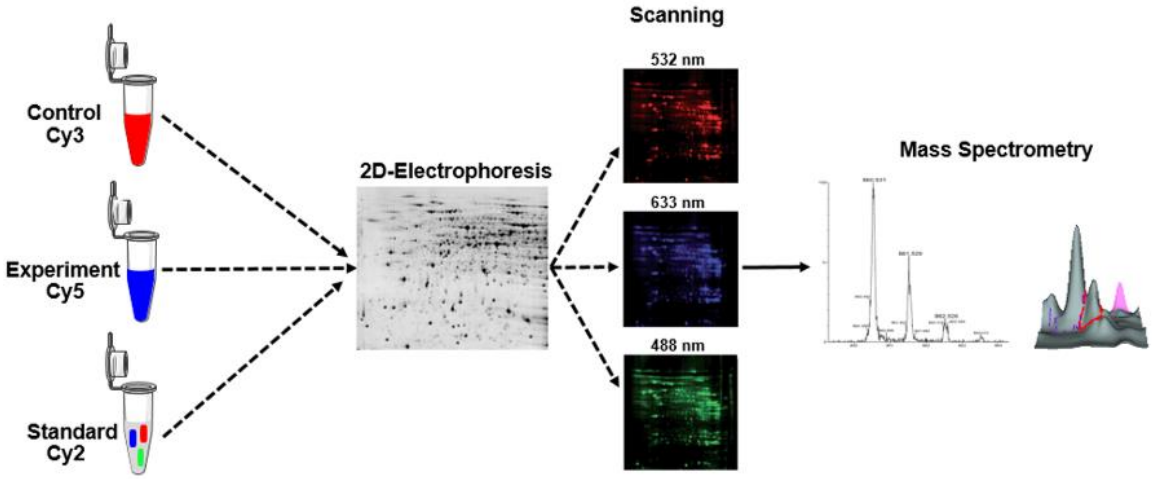

Figure 10. 2D-DIGE work flow. Samples are labelled with different cyanine dies: Cy3, Cy5 and Cy2, and then mixed and separated in the same 2D-gel taking into account the molecular weight and PI; the internal standard is prepared by mixing samples in the same proportion. After 2D-electrophoresis, the resulting gel is resolved by specific fluorescent excitation for each dye. Each protein pool detected as differentially expressed and/or modified is picked to perform mass spectrometry, which together with bioinformatics will identify and characterize the corresponding peptide (adapted from Debasish *et al.*, 2013).

2.3.1 Preparation of total protein extracts

Four replicas composed by one hundred L3 eye imaginal discs were prepared for the following genotypes: Elav-Gal4, UAS-mCD8::GFP and Elav-Gal4, UAS-mCD8::GFP ; ; *stg* RNAi, grown at 29ºC. The eye discs were dissected in 1X PBS and kept in a solution containing 1X phosphatase and 1X protease inhibitors in 1X PBS, during the dissection process. After this, the PBS solution was discarded, samples were frozen in liquid nitrogen and kept at -80ºC. To obtain total protein extracts, each sample was resuspended in a solubilization buffer (TS) containing 4% CHAPS, 7M urea, 2M Thio Urea and 200 mM DTT (1µl per disc, so 100µL per replica). Then, samples were centrifuged at 13 000 rpm for 10 min at 4ºC and the supernatant was sent to the Proteomics and Biochemistry Unit at the Andalusian Centre for Developmental Biology (CABD, Seville), where the remaining steps of 2D-DIGE were performed.

At CABD, protein extracts were cleaned using the 2-D Clean-up Kit (GE Healthcare), following the manufacturer's instructions. The final pellet was resuspended in 30µL of TS in 30mM of Tris-HCL up pH 9.7, leaving the protein extracts with a final pH of 8.5. The pellet was still centrifuged to remove any insoluble particle. Then, the protein content was quantified using the RC DC Protein Assay kit (BioRad). The minimal amount of protein to perform this experiment is 50µg for Cy3 or Cy5, and 25µg for Cy2; in our samples only had 60µg of total protein per genotype. Despite this, the experiment was carried out. For the labelling of samples with the cyanine dyes, 30µl of the total protein were used to label with Cy3 or Cy5, and 15µl were labeled with Cy2; the fluorophore ratio used in this labelling was 8pmoles/µg (following the manufacturer's instructions). The rehydration was performed for 20h without the samples. For the first dimension (isoelectric focusing, IEF), samples were introduced into the system through the cup loading method using strips with 24 cm and pH 3-10, in a nonlinear gradient, and the IEF program was: step-n-hold 3h 500V, gradient 7h 1000V, gradient 3h 8000V, and step-n-hold 5h36min at 8000V (total voltage – 58742 Vhr). After this first dimension, strips were equilibrated in an equilibration buffer containing 6M Ureia, 75mM Tris-HCL pH 8.8, 30% glycerol and 2% SDS, and the second dimension was carried out using 12,5% polyacrylamide. Finally, gels were scanned to detect fluorescence, and then were analyzed using the DeCyder v7.0 software. To quantify each protein spot the following filters were established: t-test filter, which only accepts values lower than 0.05; filters that only accept proteins present in both gels and with differences lower than -1.5 or bigger than 1.5.

2.4 Scanning electron microscopy (SEM)

Female flies were dehydrated through an ethanol series (25%, 50%, 75% and 100%), overnight each step and at RT. Then, they were incubated twice with 15µl of hexamethyldisilazane (HMDS) for 30 min and air-dried overnight at RT. Flies were mounted into SEM stubs (Agar Scientific) using araldite, and were coated with an Au/Pd film through Sputter Coater equipment. The SEM/EDS exam was performed using a high-resolution environmental scanning electron microscope with X-ray microanalysis and electron backscattered diffraction analysis – Quanta 400 FEG ESEM/EDAX Genesis X4M.

2.5 Statistics

The number of Repo-positive cells in the basal region of the eye disc (without consider cells in the OS) was counted using the ImageJ® plugin Cell Counter. A Student T-test was performed to compare samples and the significant differences were assessed at a 95% confidence interval. Graph was made using GraphPad Prism 6®.

3. Results

3.1 *stg* is required during eye development

Previous results from the lab (unpublished data) show that the protein phosphatase (PPase) encoded by *stg* is expressed in differentiated cells of the fly visual system (Figure 8 A, asterisks), but its function in this non-dividing context remains elusive. To address the function of *stg* in these post-mitotic cells we started by performing a broad analysis using GMR-Gal4 as a driver to promote downregulation of *stg.* This driver promotes the expression of the RNAi in all cell types posterior to the MF (Freeman, 1996). In control flies, GMR-Gal4, we observed the characteristic highly organized and regular array of the fly retina (Figure 11 A, C), while in GMR-Gal4>*stg* RNAi flies we observed a strong rough eye phenotype (Figure 11 B, D). This phenotype is characterized by an apparent reduction of the eye size and a severe disruption of the retina lattice, where ommatidia fusions, loss of bristles and apoptotic blisters are readily observed (encircled in Figure 11 B, D). These flies were observed during approximately fifteen days and the phenotype do not become worse with time. We also observed that GMR-Gal4>*stg* RNAi females showed a strongest phenotype (Figure 11 D). This is most likely due to fact that GMR-Gal4 is inserted in the X chromosome. Altogether, these findings suggest that Stg plays an important function during the development of the cell-types posterior to the MF.

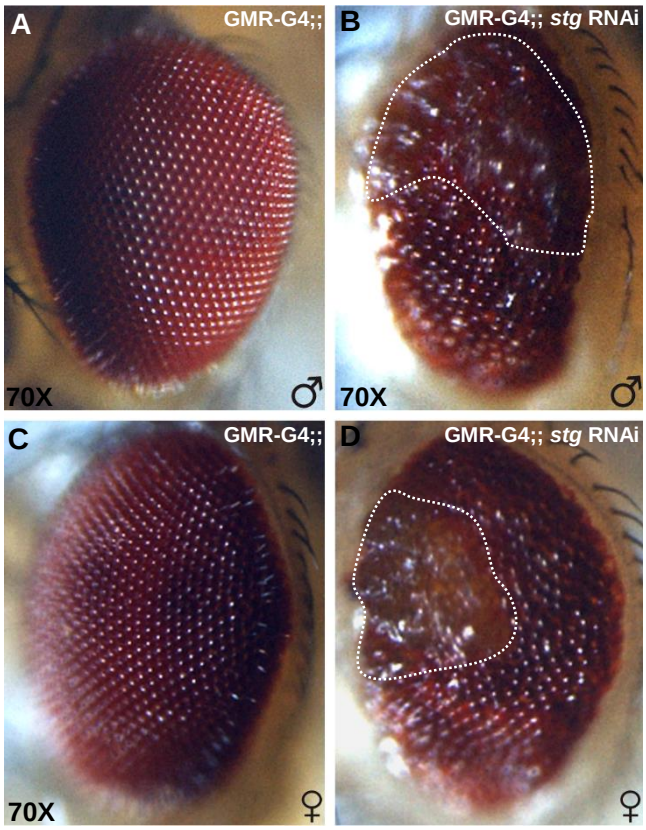

Figure 11. Downregulation of *stg* in all cell types posterior to the MF leads to a strong rough eye phenotype. The GMR-Gal4 driver was used to promote *stg* downregulation in all cell-types posterior the MF, through the use of an RNAi transgene. GMR-Gal4 (A, C) was used as control. Representative samples of adult fly heads are shown (A - D). Upon *stg* downregulation, the highly regular ommatidia array is severely disrupted (B, D); an apparent reduction of the eye size, ommatidia fusions and apoptotic blisters are readily observed (encircled in B, D). Females (D) display the strongest phenotype upon *stg* downregulation.

3.2 Characterization of *stg* function in photoreceptor neurons

3.2.1 Downregulation of *stg* in photoreceptors leads to an adult rough eye phenotype

At the differentiated region of the eye disc (posterior to the MF) there are two different cell types: PR-cells and accessory cells organized around them. The previous results suggested that Stg is required during the development of these cell types. However, Stg function may be important for both cell types or for only one. To clarify this question we decided to use the driver line Elav-Gal4, which is expressed in PR-cells (Sink *et al.*, 2001) and in neuroblasts of the OL (Berger *et al.*, 2007). Thus, using this driver we only promote *stg* downregulation in PR-cells of the eye imaginal disc. The adult fly retina was analyzed through scanning electron microscopy (SEM). This high-resolution assay showed that upon *stg* downregulation, the characteristic highly organized retina was severely disrupted, presenting ommatidia fusions, ommatidia with different sizes and loss of bristles (Figure 12 C, D). We also observed that Elav-Gal4>*stg* RNAi flies at 25ºC (Figure 12 C) hatched but they died approximately two days later, while at 29ºC (Figure 12 D) they die during pupa stages. Although no significant differences were detected on the retina by SEM analysis, these observations suggest that the consequences of *stg* downregulation at 29ºC are worst, which was expected since higher temperatures increase the activity of GAL4 and hence the expression of the RNAi (Duffy, 2002). All these findings suggest that *stg* plays an important function during PR development.

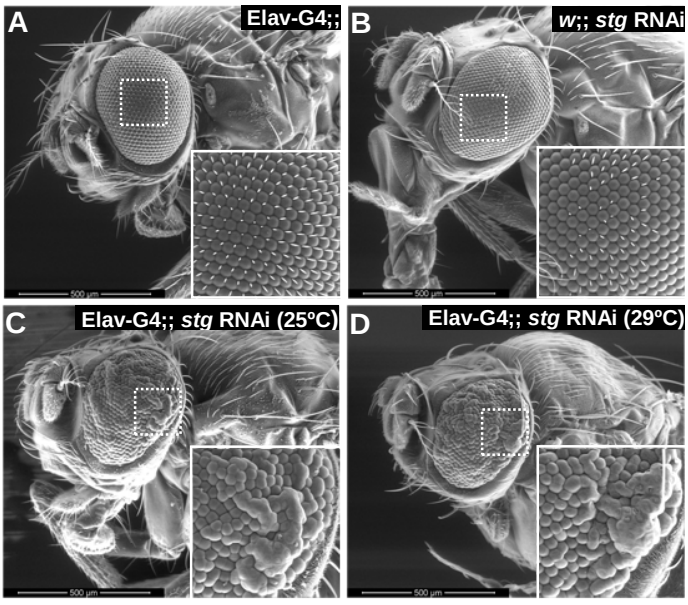

Figure 12. Scanning electron microscopy analysis of adult fly retinas upon *stg* downregulation. The Elav-Gal4 driver was used to promote *stg* downregulation in PR neurons using the RNAi transgene. Elav-Gal4 (A) and the RNAi (B) lines were used as controls. Representative samples of adult fly heads are shown (A - D). Insets from the region defined by the dashed square line are shown (A - D). Downregulation of *stg* disrupts severely the regular array of ommatidia organization; ommatidia of different sizes, ommatidia fusions and loss of mechanosensory bristles are easily observed (C, D).

To understand if high levels of *stg* affect the normal retina organization we used Elav-Gal4 as a driver to promote *stg* overexpression in PR-cells through the use of a UAS-*stg*. We analyzed adult fly heads of Elav-Gal4>*stg* and no modifications on the retina lattice were detected (Figure 13 B). This result suggests that high levels of *stg* do not disturb the retina organization and structure.

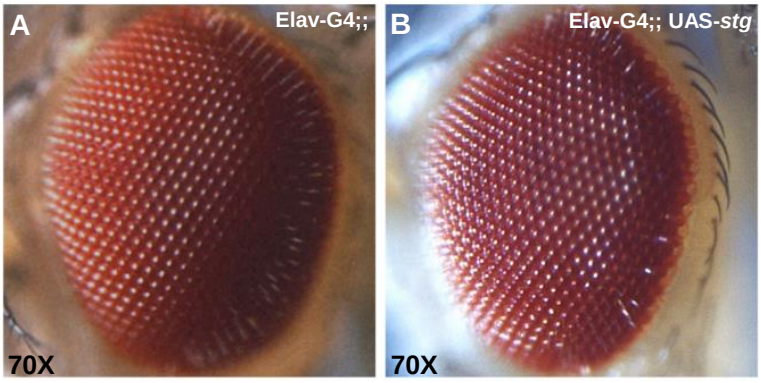

Figure 13. Overexpression of *stg* in PR-cells did not affect retina organization. Elav-Gal4 driver was used to promote *stg* overexpression in PR-cells through an UAS-*stg* transgene. Elav-Gal4 (A) was used as control. Representative samples of adult fly heads are shown (A - B). No modifications on the retina lattice were detected upon *stg* overexpression (B).

A Stg-GFP line was used to analyze Stg expression pattern in PR-cells during larval stages. Specifically, we analyzed L3 eye imaginal discs since is during this stage that the ommatidia pattern and PR differentiation occur (Ready *et al.*, 1976). In this construct, Stg is expressed as a GFP protein fusion from the endogenous promoter, allowing to know its dynamic distribution along the eye disc (Morin *et al.*, 2001). In L3 eye imaginal discs labeled with Elav, which identify the PR-nuclei, we observed that Stg is highly expressed in retinal precursors and in the SMW. After the SMW, we detected that some Elav-positive cells are GFP-positive (Figure 14 A, A', yellow arrows), meaning that not all PR-cells of the ommatidia express Stg. Around the PRs, we detected Elav-negative, GFP-positive cells (Figure 14 A, A', white arrow), which could mean that accessory cells, which are known to surround PR-cells, also express Stg.

We next evaluated the consequences of *stg* downregulation during L3 to understand which are the processes and/or structures whose impairment lead to the adult rough phenotype observed. For this, L3 eye imaginal discs were stained with specific antibodies: Elav, Rho/Phall to label actin membranes, and GFP to visualize Stg expression. Stg-GFP was used as control (Figure 14 A – C'). In a cross-section view, the PR-nuclei are organized (Figure 14 A'', lines) and maintained in an apical position of the tissue (Figure 14 B, C'). Upon *stg* downregulation (Figure 14 D-F'), the parallel array of ommatidia organization is

disrupted (Figure 14 D'', lines) and ommatidia of different sizes are detected (Figure 14 D'', arrows). The nuclei of PR-cells also fail to maintain their apical position and fall into the basal surface of the neuroepithelium (Figure 14 F', arrows). We also detected that upon downregulation, PR-cells localized posterior to the SMW fail to express Stg (Figure 14 B, E, arrowheads), showing that *stg* was efficiently downregulated. Taking together, these data suggest that Stg is only expressed in some PR-cells, being required during eye development for the apical maintenance of PR-nuclei and ommatidia organization.

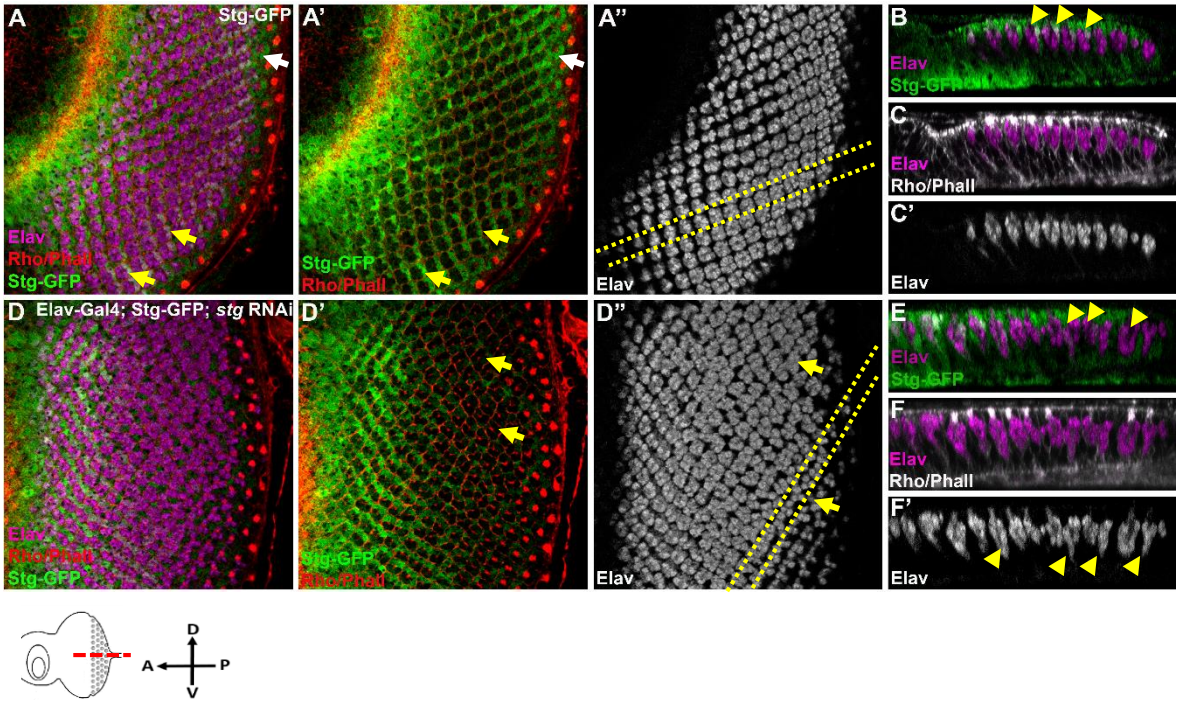

Figure 14. Upon *stg* downregulation, PR-nuclei become disorganized and fail to maintain in the apical surface on the eye imaginal disc. The Elav-Gal4 driver was used to promote *stg* downregulation in PR-neurons (A - F'). A Stg-GFP line was used to visualize Stg expression (green) in PR-cells (A - C'). L3 eye imaginal discs from Stg-GFP were used as control (A – C'). Apical views (A, A', A'', D, D', D'') and cross-sections (B, C, C', E, F, F') are shown. L3 eye imaginal discs stained for Elav (magenta) to label PR-nuclei, Rho/Phall (red) to identify actin membranes, and GFP (green) to reveal Stg expression. Upon *stg* downregulation, the highly organized array of ommatidia is disrupted (D'', lines); ommatidia with an abnormal number of PRs are observed (D'', arrows). Cross-sections showing that upon *stg* downregulation PR-nuclei fail to maintain the apical position (F', arrowheads). PR-nuclei fail to express Stg upon *stg* downregulation (E, arrowheads). (A, anterior; P, posterior; V, ventral; D, dorsal; dashed line identify the direction of cross-sections).

3.2.2 *stg* appears to be required for specification of cone cells

Our next question was to understand if *stg* is required for cell specification in the developing eye since the disorganization observed upon *stg* downregulation could be due to an impaired cell fate. For this, L3 eye imaginal discs were labeled with two differentiation markers that label two different PR-cell group, Rough (Ro) and Prospero (Pros). In WT eye imaginal discs, Ro is expressed in R2, R3, R4 and R5 (Kimmel *et al.*, 1990). In control discs (Figure 15 A, A'), we can clearly see that PR-cells express Ro in a patterned manner. Although we did not detect any changes in Ro express pattern upon *stg* downregulation (Figure 15 B, B'), we cannot conclude that these PR-cells are being normally specified. It is possible only one PR-cell type was specified in twice (or more) per ommatidia generating a similar pattern as control samples.

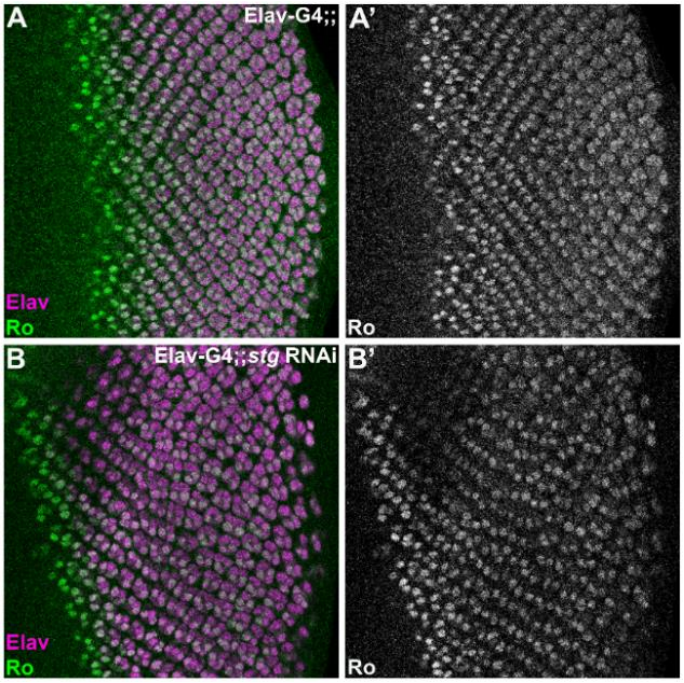

Figure 15. Ro expression pattern was not modified upon *stg* downregulation in PR-cells. L3 eye imaginal discs labeled for Rough (Ro, green) to identify R2, R3, R4 and R5 cells, and Elav (magenta). Elav-Gal4, UAS-mCD8::GFP (A, A') was used as control. Apical views are shown (A - B'). No changes were detected on Ro expression pattern upon *stg* downregulation (B, B').

In WT eye imaginal discs, Pros is expressed in the nucleus of the R7 equivalence group (R1, R6, R7 and cone cells) (Kauffmann *et al.*, 1999). Upon *stg* downregulation, we detected extra Pros-positive, Elav-negative cells, when comparing to control samples (Figure 16 B'). These extra cells could be cone cells, meaning that their specification upon *stg* downregulation may be disrupted in a manner that extra cells are being specified. Taking together, our findings suggest that Stg function could be required for the proper specification of cone cells.

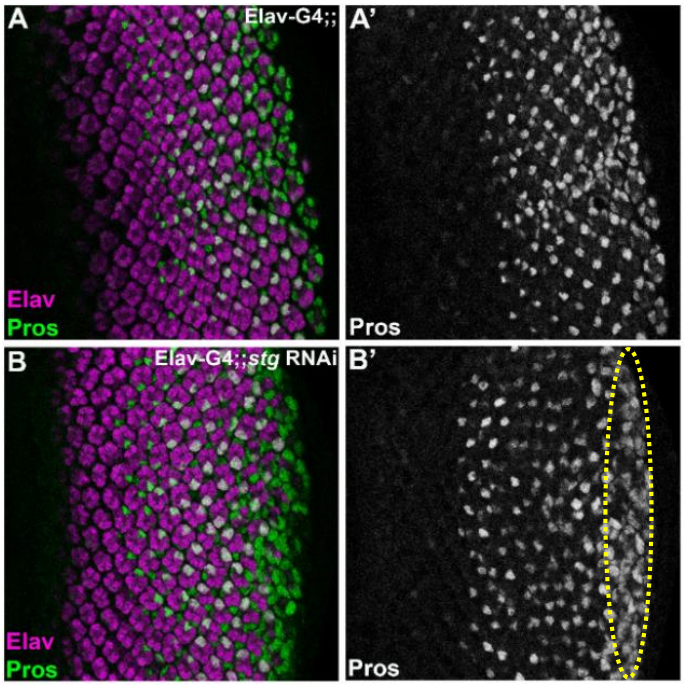

Figure 16. *stg* appears to be required for specification of cone cells. L3 eye imaginal discs stained for Prospero (Pros, green) to identify the R7 equivalence group, and Elav (magenta). Elav-Gal4, UAS-mCD8::GFP (A - A') was used as control. Apical views are shown (A - B'). Downregulation of *stg* disrupts Pros expression pattern; extra Pros-positive, Elav-negative cells were detected (encircled in B').

3.2.3 *stg* is required for cytoskeleton organization

Cytoskeleton plays an essential role during organ development providing cellular shape and support, which is important for compartmentalization and polarity (reviewed in Dent *et al.*, 2011; Coles & Bradke, 2015). Previous results showed that in the absence of *stg,* PR-nuclei fail to maintain their apical position in the neuroepithelium and the adult retina becomes highly disorganized. Taking this into account, we next evaluated if there was any disruption in the structure and organization of both neuronal actin and MT cytoskeleton upon *stg* downregulation. To analyze the actin cytoskeleton organization, the reporter line UAS – Lifeact::RFP, which expresses an actin-binding peptide fused to RFP, was used to identify filamentous actin (F-actin) (Riedl *et al.*, 2008). This line was initially crossed with Elav-Gal4 and then downregulation of *stg* in PR-cells was performed through the use of the RNAi transgene. In an apical view, we clearly observed that F-actin clusters at the center of the ommatidia (Figure 17 A); in cross-sections, F-actin is localized apically in a very organized manner and along the axons (Figure 17 B', arrows). However, upon *stg* downregulation we observed that F-actin distribution becomes disorganized (Figure 17 C, arrow) and apparently fails to spread along the axons (Figure 17 D', arrow).

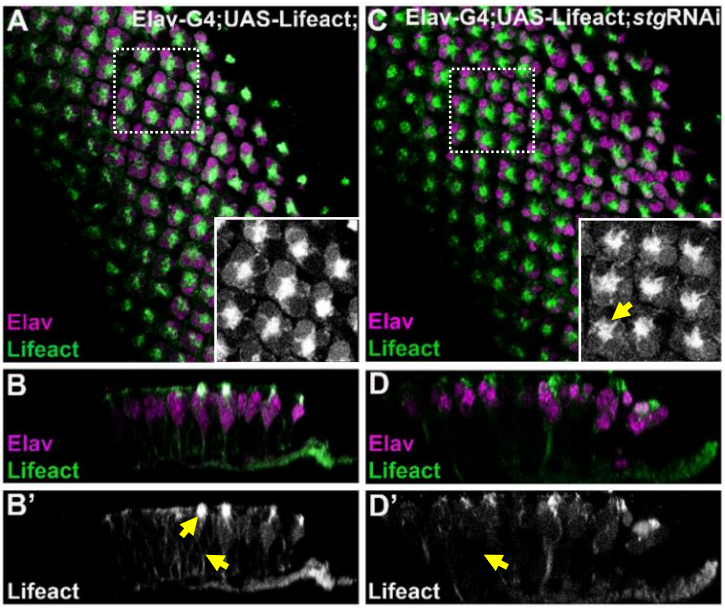

Figure 17. **Downregulation of *stg* impairs actin cytoskeleton organization.** L3 eye imaginal discs stained for Elav (magenta), and Lifeact (green) to identify filamentous actin. Elav-Gal4; UAS-Lifeact::RFP was used as control (A - B'). Apical views (A, C) and cross-sections (B, B', D, D') are shown. Upon *stg* downregulation (C - D'), F-actin distribution at the center of the ommatidial cluster is disrupted (C, arrow). Cross-sections showing that upon *stg* downregulation F-actin appears to fail to localize along the axons (D', arrow).

To evaluate the MT cytoskeleton, L3 eye imaginal discs were labeled for the MT-associated protein Futsch. In controls samples, Futsch accumulates in the central region of the ommatidia, extending from the cell body (Figure 18 A, B) and along the axons (Figure 18 B', arrow). Upon *stg* downregulation, we observed an abnormal accumulation of Futsch surrounding the cell body (Figure 18 C). In cross-sections we detected that Futsch accumulates apically and fails to localize along the axons (Figure 18 D', arrows). Taking together, our results suggest that *stg* is required for cytoskeleton organization in the developing PR-cells.

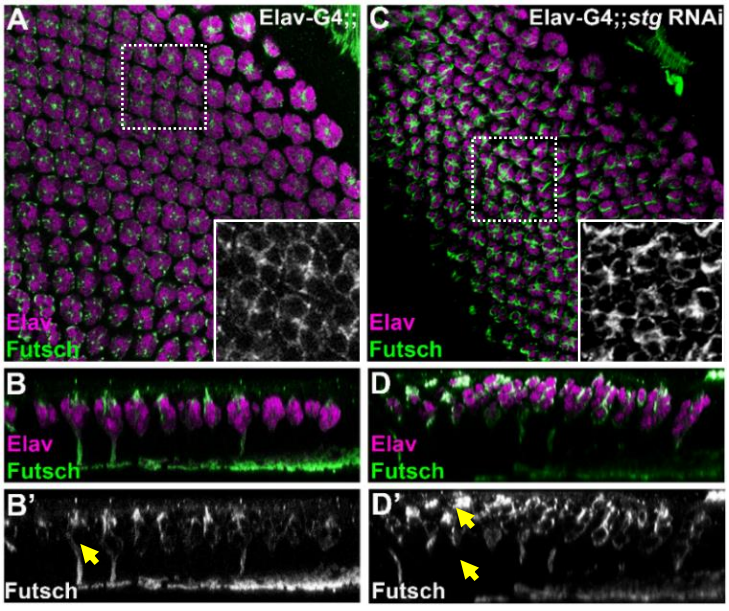

Figure 18. Downregulation of *stg* leads to an abnormal accumulation of Futsch in PR-cells. L3 eye imaginal discs stained for Elav (magenta) and the MT-associated protein Futsch (green). Elav-Gal4, UAS-mCD8::GFP (A - B') was used as control. Apical views (A, C) and cross-sections (B, B', D, D') are shown. Upon *stg* downregulation, an abnormal accumulation of Futsch in the PR-cell body is observed (C); cross-sections showing that Futsch accumulates apically and fails to localize along the axons (D', arrows).

3.2.4 *stg* downregulation impairs axonal integrity and projection into the optic lobe

We next evaluated if the cytoskeleton impairment observed upon *stg* downregulation has any effect on axonal integrity and subsequently on the projection into the OL. For this, L3 eye imaginal discs of Elav-Gal4; UAS-Lifeact::RFP were stained for Futsch to identify MTs. In control samples, PR-axons display a homogenous and regular thin structure (Figure 19 A', A''). Upon *stg* downregulation, we observed that the axonal structure was disrupted, showing a beads-like structure and formation of bundles (Figure 19 B', B'').

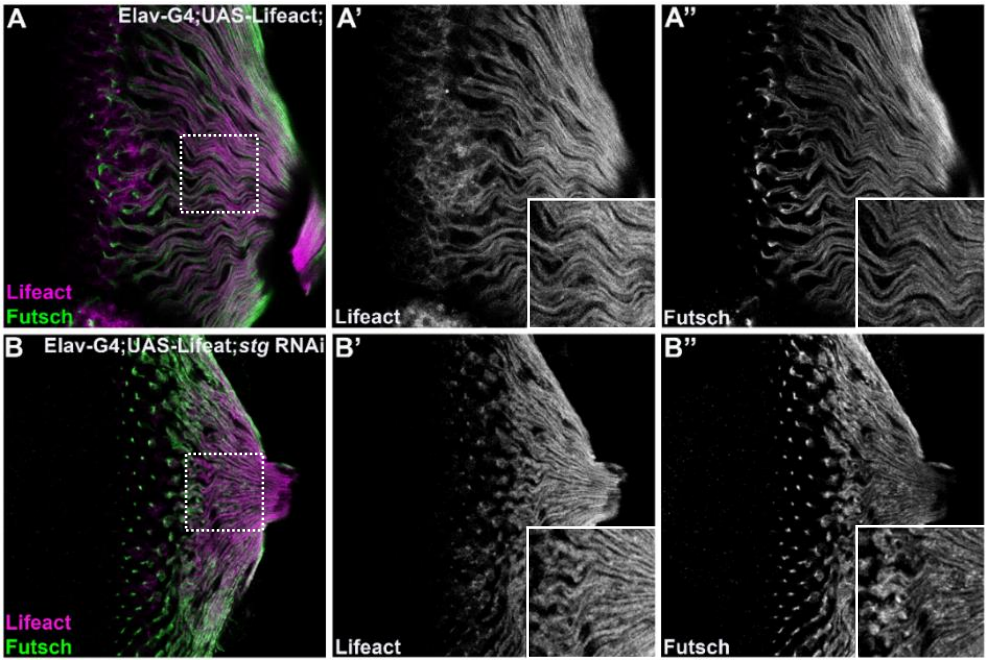

Figure 19. Analysis of axonal integrity upon *stg* downregulation. L3 eye imaginal discs stained for Lifeact (magenta) and Futsch (green) to analyze the integrity of PR-axons. Elav-Gal4; UAS-Lifeact::RFP (A - A'') was used as control. Basal views of the neuroephitelium (A - B'') are shown. Upon *stg* downregulation (B - B''), the axonal structure is disrupted showing aggregates (swellings) and bundles (B', B'').

During PR-differentiation, nuclei migrate into the apical surface of the eye disc and axons extend into specific regions of the OL (Fan & Ready, 1997). Since previous experiments showed that in the absence of *stg* PR-nuclei fail to maintain their apical position and the axonal structure is impaired, we decided to analyze if in these conditions PR-cells project properly into the OL. The Elav-Gal4 driver has a pan-neuronal expression (Berger *et al.*, 2007) so, to address this question we used GMR-Gal4 as a driver, which does not affect the OL and brain development. For that, L3 eye imaginal discs were labeled for Futsch to identify the axonal network. In controls samples, PR-cells project their axons in parallel

bundles into the lamina and medulla neuropils of the OL (Figure 20 A, A'). Upon *stg* downregulation, we detected that PR-cells project irregularly into the lamina and fail to project into the medulla (Figure 20 B, B', arrow). Thus, our data suggest that *stg* is required during eye development to confer a proper axonal structure of PR-cells and hence for their projection into the OLs.

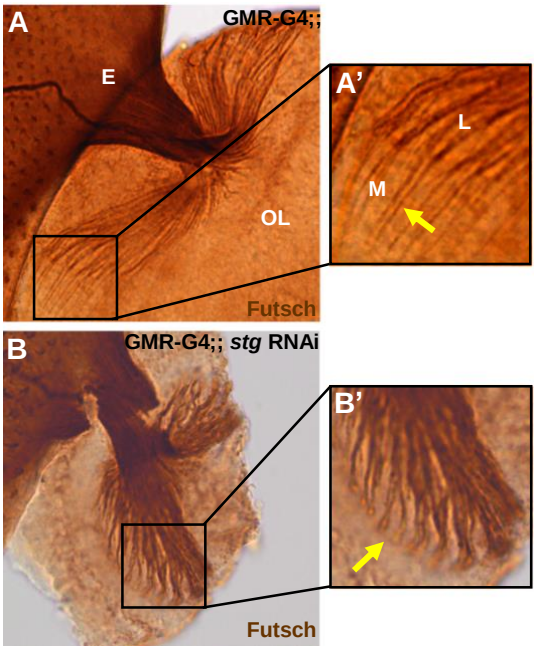

Figure 20. Analysis of PR-axon projections into the optic lobe upon *stg* downregulation. GMR-Gal4 driver (A, A') was used to promote *stg* downregulation in all differentiated cells of the eye, using the RNAi transgene. L3 eye imaginal discs stained for Futsch (brown) to evaluate axonal projection into the OL. The basal region of the eye (E) and the OL are shown (A - B'). In control samples, PR-cells project on a regular manner into the lamina (L) and medulla (M) of the OL (A, A', arrow). Upon *stg* downregulation, PR-cells project irregularly into the lamina and fail to project into the medulla (M) (B, B', arrow).

3.3 The requirement of *stg* in accessory cells

By using the Stg-GFP line, we observed that accessory cells also express Stg (Figure 14 A, A', white arrow). Thus, we decided to determine if *stg* is required during development of these cell types. To address this question, we used the driver Lozenge-Gal4 (Lz-Gal4) which has been described to promote the expression of transgenes in the R7 equivalence group and in pigment cells (Crew *et al.*, 1997). As previously reported, control adult flies (Figure 21 A) display a highly regular and organized retina. However, we observed that *stg* downregulation induced a smooth disruption of retina, where ommatidia fusions and loss of bristles are detected (Figure 21 B, C). This experiment was also performed at different temperatures and we detected a stronger phenotype at 29ºC (Figure 21 C). In both conditions, Lz-Gal4>*stg* RNAi flies were observed during approximately fifteen days and phenotypes did not become worse, similar to the observed upon *stg* downregulation in PR-cells. Thus, since this driver line also promotes RNAi expression in some PR-cells, the phenotype observed can be due to *stg* downregulation in these PR-cells and/or caused by the requirement of *stg* in accessory cells.

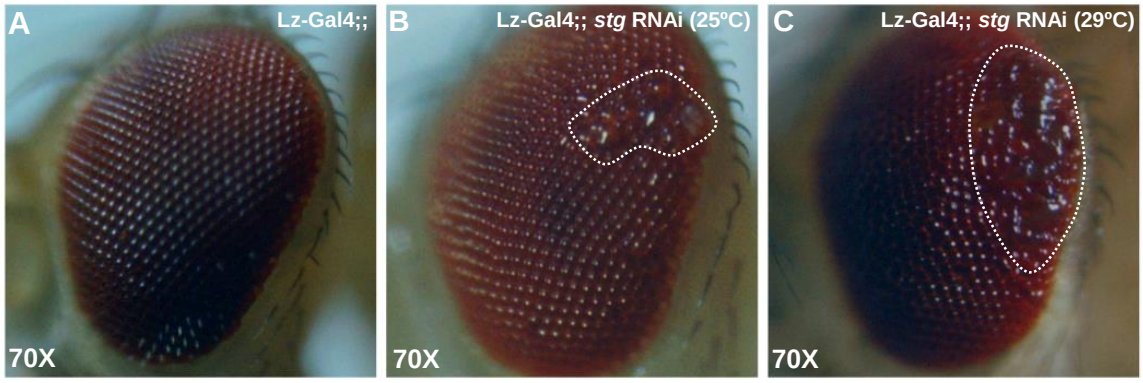

Figure 21. Downregulation of *stg* in R7 equivalence group and pigment cells leads to a smooth rough eye phenotype. Lz-Gal4 was used to promote *stg* downregulation in R1, R6, R7 and accessory cells through the use of the RNAi transgene. Lz-Gal4, UAS-mCD8::GFP (A) was used as control. Representative samples of adult fly heads are shown (A - C). *stg* downregulation (B, C) leads to a slightly disruption of retina specifically in more posterior regions of the eye; ommatidia fusion and loss of bristles are observed (encircled in B and C). *stg* LOF phenotype was worst at 29ºC (C).

To clarify the requirement of *stg* in accessory cells we next used another driver line, Sparkling-Gal4 (Spa-Gal4), which is described as specific for accessory cells (Fu & Noll, 1997). We started to confirm the Spa-G4 expression in the eye disc using an UAS-GFP. For that, late L3 eye imaginal discs of Spa-Gal4 ; UAS-GFP were labelled for Elav and Cut to identify PR and cone cells, respectively (Figure 22 A - A'). With this experiment we observed that there were Cut-positive cells which are not GFP-positive (Figure 22 A', arrows), meaning that Spa-Gal4 is not driving UAS-GFP in all cone cells. We also detected an overlap between Elav and GFP (Figure 22 A, arrows), which suggest that Spa-Gal4 is also driving GFP expression in PR-cells. Therefore Spa-Gal4 driver is not specific for accessory cells, the role of *stg* in this ommatidia cell-type remains elusive.

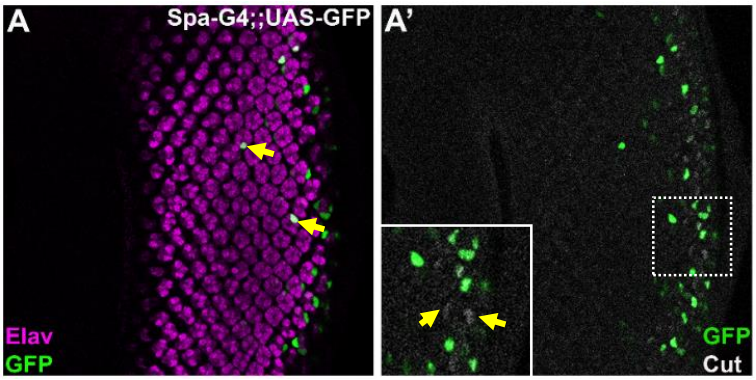

Figure 22. Spa-Gal4 promotes GFP expression in some cone and PR-cells. Spa-Gal4 ; UAS-GFP was used to determine if Spa-Gal4 driver is specific for accessory cells. Late L3 eye imaginal discs stained for Elav (magenta), GFP (green), and Cut (white) to identify cone cells. Apical views (A - A') are shown. An overlap Elav - GFP was detected (A, arrows). Some Cut-positive, GFP-negative cells were detected (A', arrows).

3.4 The potential role of *stg* in neurodegeneration

3.4.1 *stg* downregulation induces an abnormal accumulation of Cyclin B in photoreceptors

Many studies have demonstrated that under neurodegenerative conditions, post-mitotic neurons abnormally re-express several cell cycle markers (Husseman *et al.*, 2000) and replicate their DNA (Yang *et al.*, 2001). This abnormal expression of cell cycle markers, such as Cyc B, has been correlated with a cell cycle re-entry, which ultimately induce neuronal death (Busser *et al.*, 1998; Yang *et al.*, 2003). Since *stg* downregulation in PR-cells results in a phenotype that resembles neurodegeneration, we decided to analyze Cyc B expression in the absence of *stg*. To address this question, L3 eye imaginal discs were stained for Elav and Cyc B. In controls samples (Figure 23 A, B''), we observed that cells performing the SMW express Cyc B; posterior to the SMW, Cyc B expression is reduced (Figure 23 A, A'). However, upon *stg* downregulation we clearly detected an upregulation of Cyc B in accessory cells (Figure 23 C', red arrow) and that some PR-cells posterior to the SMW accumulate Cyc B (Figure 23 C', yellow arrow; D, arrows). This observation could represent an attempt of PRs to re-enter the cell cycle or an impairment at the protein degradation machinery.

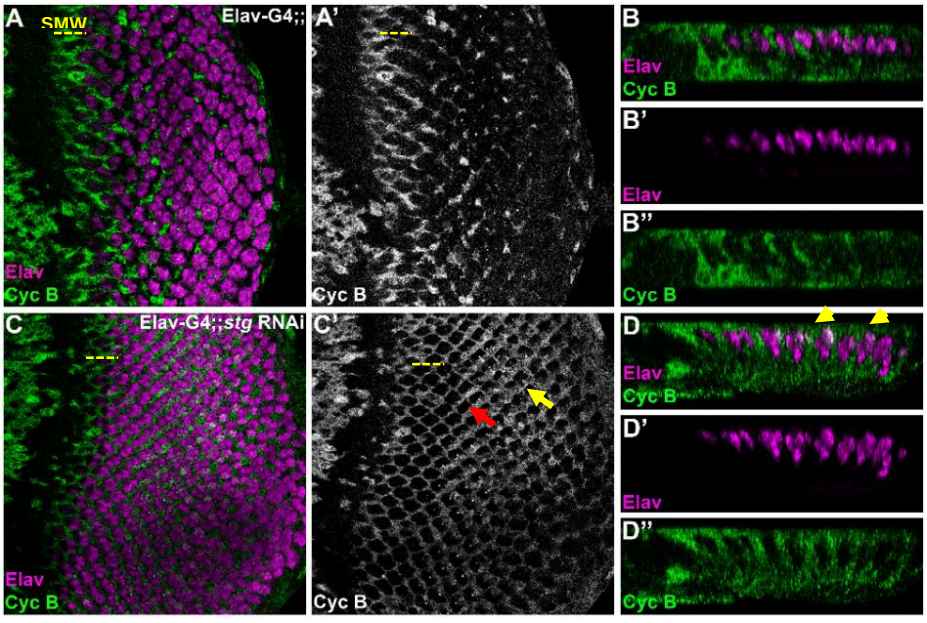

Figure 23. *stg* downregulation induces an abnormal accumulation of Cyc B in PR-cells. L3 eye imaginal discs stained for membrane CD8-GFP (green), and Cyc B (magenta) (A - D''). Apical views (A, A', C, C') and cross-sections (B, B', B'', D, D', D'') are shown. Elav-Gal4, UAS-mCD8::GFP (A - B'') was used as control. In these discs, Cyc B is expressed in cells performing the SMW (A, A', arrows). Upon *stg* downregulation, Cyc B is upregulated in accessory cells (C', red arrow) and an abnormal accumulation in PRs was also detected (C', yellow arrow). Cross-sections showing the accumulation of Cyc B in PR-cells (D, arrows).

3.4.2 *stg* downregulation does not induce photoreceptor cell death during larval stages

As previously referred, the rough eye phenotype caused by *stg* downregulation in PR-cells resembles a neurodegenerative phenotype. Previous results showed that during larval stages this phenotype is characterized by defects in several cell structures and processes, such as cytoskeleton organization/structure and nuclei positioning, which could lead to unstable PR-cells. With an impaired projection into the OL, PR-axons fail to establish synaptic contacts with lamina and medulla neurons, which could lead to neurodegeneration. Taking all these evidences into account, we decided to analyze if PR-axons are dying upon *stg* downregulation. For this, L3 eye imaginal discs were stained for Elav, and Caspase 3 to identify dying PR-cells. In controls, w^{1118} and Elav-Gal4, we did not detect cell death markers in PR-cells (Figure 24 B, C). Upon *stg* downregulation, we also failed to detect caspase 3-positive cells (Figure 24 D).

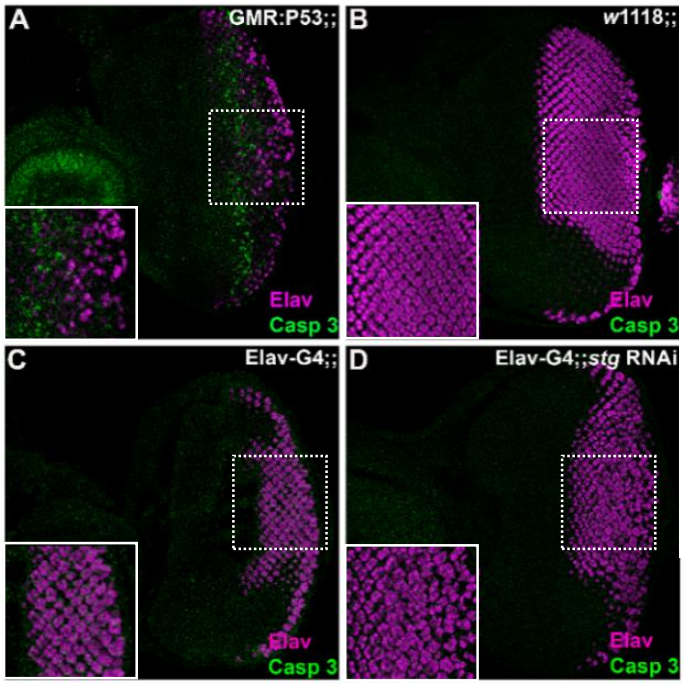

Figure 24. Downregulation of *stg* did not induce photoreceptor cell death during larval stages. L3 eye imaginal discs stained for Elav (magenta), and Caspase 3 (green) to analyze cell death in PR-cells. Apical views are shown (A - D). GMR: P53 (A) was used as positive control, showing cell death in PR-cells. w^{11118} (B) and Elav-Gal4, UASmCD8::GFP (C) were used as WT controls, where no cell death was identified. No Elav-positive, caspase 3-positive cells were detected upon *stg* downregulation (D).

Disruption of the inner-nuclear membrane also correlates with cell death (Buendia *et al.*, 1999). Therefore, we evaluated its integrity upon *stg* downregulation. For that, L3 eye imaginal disc were stained for Elav, and Lamin to identify the nuclear membrane of PR-cells (Krohne & Benavente, 1986). We observed that the intact and continuous inner-nuclear membrane observed in control samples (Figure 24 A, A') was maintained upon *stg* downregulation (Figure 25 B, B'). Taking together, our results suggest that cell death induced by *stg* downregulation does not occur during larval stages.

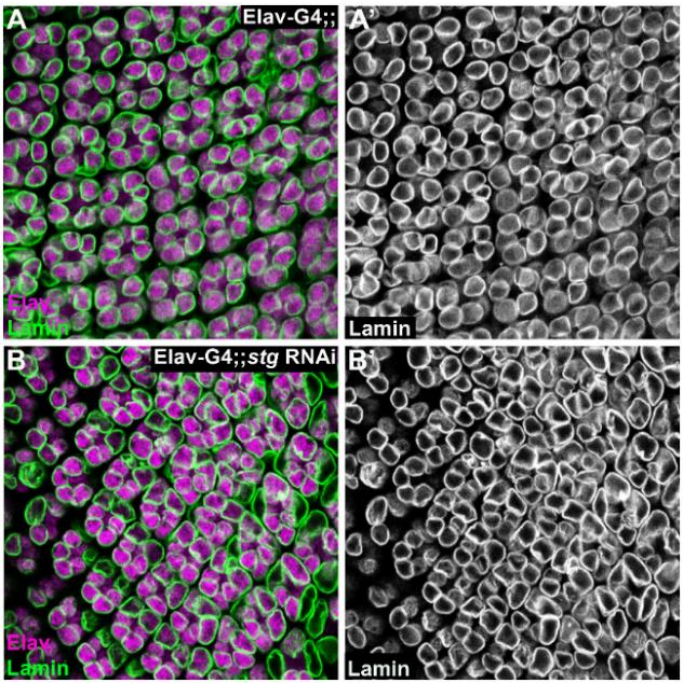

Figure 25. Upon *stg* downregulation, the integrity of the inner-nuclear membrane of PRs was maintained. L3 eye imaginal discs stained for Elav (magenta), and Lamin Dm0 (green) to identify the inner-nuclear membrane of PR-cells. Elav-Gal4, UASmCD8::GFP (A, A') was used as control. Apical views are shown (A - B'). No alterations in the inner-nuclear membrane of PR-cells were detected upon *stg* downregulation.

3.4.3 Downregulation of *stg* does not promote glia overmigration into the eye imaginal disc

Glial cells play a critical role in the development and maintenance of the nervous system (reviewed in Shaham, 2005). In rats, glial cells are crucial to maintain the homeostasis and survival of damaged cells. After injury, microglia and astrocytes are activated, producing several growth factors and cytokines to repair the damaged tissues. However, the prolonged glial activation and excessive cytokines production are toxic to neurons, inducing neuronal death (Suzumura *et al.*, 2006). In *Drosophila*, several mutations that cause late-onset neurodegeneration have shown glial defects (Buchanan & Benzer, 1993). In mutants for *drop-dead* gene, glial cells display shortened processes, which are responsible for degeneration of lamina and PR-neurons (Buchanan & Benzer, 1993). Mutations in regulators of glia migration are also associated with glial defects. Mutations in the membrane protein spinster, for instance promote glia overactivation inducing their overmigration to regions anterior to the MF (Yuva-Aydemir *et al.*, 2011).

Taking this into account, we decided to evaluate if the neurodegeneration caused by *stg* downregulation induces any glial defect, such as overmigration onto the eye imaginal disc. To address this question, L3 eye imaginal discs were stained for Elav, membrane-GFP, and Repo to identify glial cells (Halter *et al.*, 1995). In control samples, we observed that glial cells are localized in the basal region of the eye imaginal disc along the axons

(Figure 26 A – B''). Upon *stg* downregulation, no significant differences were detected (Figure 26 C - D''). Additionally, we counted the number of Repo-positive cells in control samples and upon *stg* downregulation to understand if glial cells overmigrate onto the eye imaginal but we do not identify any significant difference (Figure 27). Thus, our data suggest that upon *stg* downregulation glial cells do not overmigrate into the eye imaginal disc.

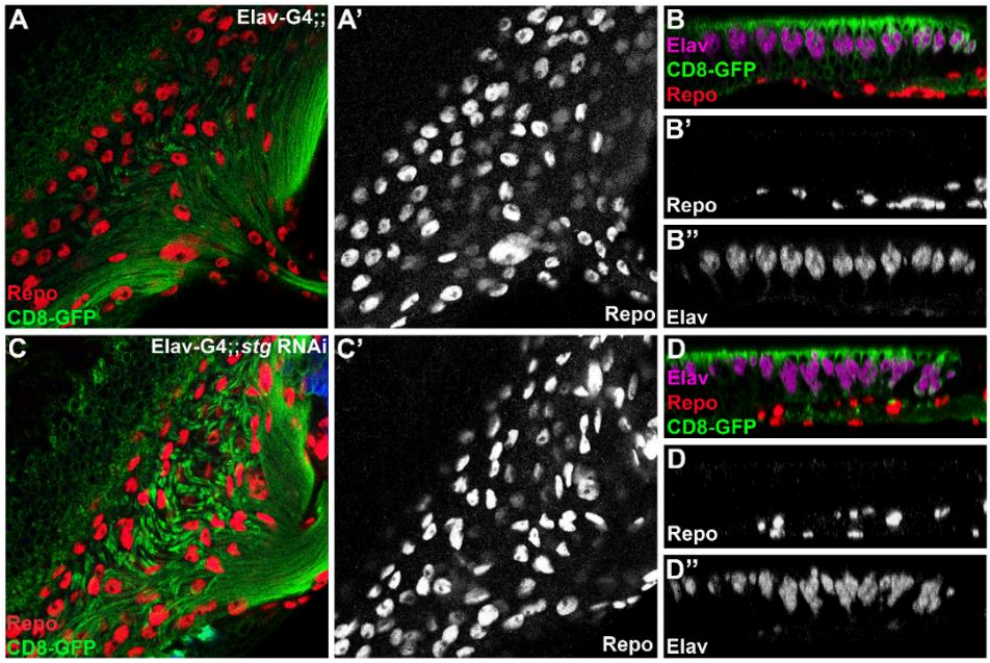

Figure 26. Analysis of Repo expression upon *stg* downregulation in PR-cells. L3 eye imaginal discs stained for Elav (magenta), membrane-GFP (green), and Repo (red) to identify glial cells. Basal views (A, A', C, C') and cross-sections (B-B'', D-D'') are shown. Elav-Gal4, UAS-mCD8::GFP (A - B'') was used as control. No significant differences were detected upon *stg* downregulation (C - D'').

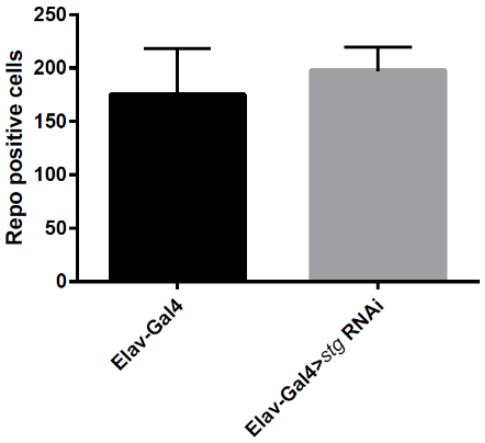

Figure 27. Quantification of Repo-positive cells before and after *stg* downregulation in PR-cells. The total Repo-positive cells in the basal region of eye were counted in control (Elav-Gal4, UAS-mCD8::GFP, n=8) and upon *stg* downregulation (Elav-Gal4, UAS-mCD8::GFP ; *stg* RNAi, n=10). Repo-positive cells within the OS were not considered. A student T-test was performed at a 95% confidence interval and no significantly differences were detected (p-value = 0.2733).

3.5 Identification of neuronal-specific substrates of Stg by 2D-DIGE

We further combined the functional analysis with a specific proteomic approach, 2D-DIGE, to identify the potential substrates of Stg in PRs. For this, total protein extracts from L3 eye-antenna imaginal discs of Elav-Gal4 and Elav-Gal4 ; *stg* RNAi were analysed. With this proteomic assay, we identified seven proteins whose expression levels were modified upon *stg* downregulation (Figure 28, Table 4). Based on the average ratio, it was possible identify different isoforms for some proteins, as it was the case of the Cuticular protein 31A (C1, C2) and the fat body protein 1 (C6, C7). This ratio also allow us to conclude that in the absence of *stg,* one isoform of the cuticular protein 31A (C1), tropomyosin I/II and the calcium ion-binding protein are upregulated.

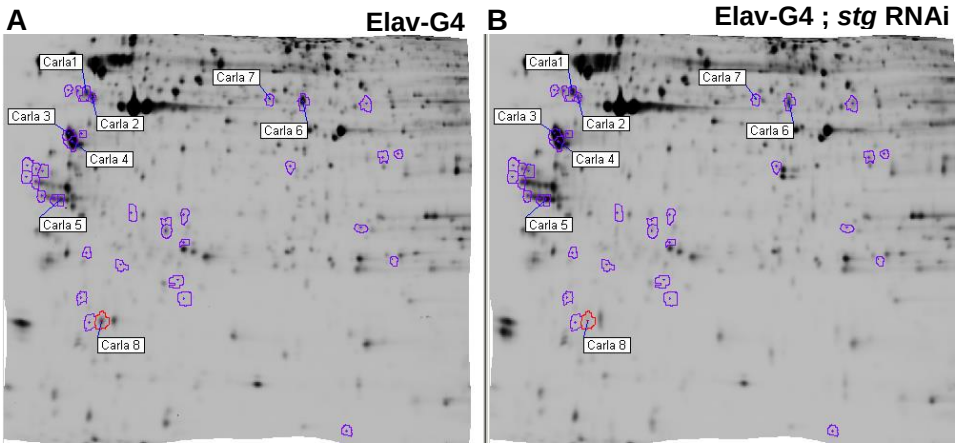

Figure 28. Identification of neuronal-specific substrates of Stg by 2D-DIGE. Total protein extracts from L3 eye discs of Elav-Gal4, UAS-mCD8::GFP (A) and Elav-Gal4, UAS-mCD8::GFP ; *stg* RNAi were used to perform 2D-DIGE. Proteins were separated based on PI and molecular weight. Several proteins were differentially expressed upon *stg* downregulation (encircled in A - B).

Table 4: Identification and characterization of the potential substrates of Stg in PR-cells identified by 2D-DIGE

Identification		T-test	Av. Ratio	pI	Mol. weight	Name
Protein AC	CG					
Q8IPD5_DROME	33302	1.80E-03	1.73	4.8	35	Cuticular protein 31A
Q8IPD5_DROME		8.40E-06	-1.77	4.8	35	
H1UUP7_DROME	4898	5.50E-04	1.62	4.3	53	Tropomyosin I
H1UUJ7_DROME		8.80E-04	1.57	4.7	33	Tropomyosin II
Q6NNE3_DROME	---	1.30E-04	1.62	4.6	23	RH35841p (Calcium ion-binding protein)
M9PFK6_DROME	17285	5.60E-06	-1.7	6.0	119	Fat body protein1
M9PFK6_DROME		2.50E-03	-1.98	6.0	119	

4. Discussion

Our results show that *stg* function is required during PR-development. Through a functional analysis we concluded that *stg* plays an important role in the apical maintenance of PR-nuclei and for ommatidia organization, contributing to a highly organized adult retina array. We also observed that *stg* is required for both neuronal actin and MT cytoskeleton organization, ensuring a proper axon structure and its projection into the OL.

4.1 *stg* is required for retina organization during eye development

Downregulation of *stg* in PR-cells induced an adult rough eye phenotype, characterized by an apparent reduction of the eye size and a highly disorganized retina (Figure 12 C and D). In L3 eye imaginal discs we observed that PR-nuclei fail to maintain their apical position (Figure 14 F'), which might be responsible for the ommatidia disorganization observed. The displacement of PR-nuclei from the apical surface could disrupt the apical/basal polarity of the developing PR-cells (Whited *et al.,* 2004), also contributing for this disorganization. The apico/basal polarity of the developing PRs could be evaluated analyzing the distribution of specific polarity complexes, such as Armadillo and PATJ (Pielage *et al.*, 2003) in L3 eye imaginal discs. In a WT condition, Armadillo is localized between the apical and basolateral membrane of PRs, while PATJ is present at the apical membrane domain (Pielage *et al.*, 2003). If Stg regulates the apical/basal polarity, we expect these markers to be displaced from the apical domain upon *stg* downregulation.

Disruptions during PR specification could also contribute to the ommatidia disorganization. The first PR-cell to be specified is R8 (Lim & Choi, 2003). Since Elav-Gal4 is only expressed from the MF onward (Berger *et al.*, 2007), downregulation of *stg* using this driver will not affect R8 specification. However, Mozer *et al.,* (1999) already reported that *stg* is not required for the onset of pattern formation. In mutants where *stg* expression is inhibited in a stripe of cells anterior to the MF (Dr^{hwy}), they observed the pattern of *ato* expression and did not identify any modification comparing to WT samples, suggesting that R8 specification is independent of *stg* function (Mozer & Easwarachandran, 1999). R2, R3, R4 and R5 are also specified in a region of the eye disc where Elav-Gal4 is not expressed (Lim & Choi, 2003). However, their recruitment and specification occurs through inductive signals emitted by R8, which could be disrupted upon *stg* downregulation.

We analyzed the specification of different cell-types of the ommatidium upon *stg* downregulation using Ro and Pros. Ro was used to label R2, R3, R4 and R5 *(*Kimmel *et al.*, 1990). We did not detect modifications in Ro expression pattern in the absence of *stg* (Figure 15 B, B'). However, we cannot conclude that individual PR-cells were normally

specified. It could be possible that only one PR-cell type was specified in twice (or more) per ommatidia, generating a similar pattern as observed in control eye imaginal discs. Labeling L3 eye imaginal discs with other markers, such as Rhomboid to analyze particularly R2 and R5 (Freeman *et al.*, 1992) and Spalt for R3 and R4 (Domingos *et al.*, 2004) might be a useful approach to clarify this question. Pros was used to label the R7 equivalence group, which is composed by R1, R6, R7 and cone cells (Kauffmann *et al.*, 1999). Upon *stg* downregulation we observed extra Pros-positive, Elav-negative cells, comparing to control samples, suggesting that cone cells were not properly specified (Figure 16 B, B'). Since Spa is only expressed in accessory cells (Fu & Noll, 1997), we can use this driver line to address the requirement of *stg* for the specification of cone cells. If downregulation of *stg* impairs the specification of cone cells in a manner that extra cells are specified per ommatidium, we expect to see a higher number of Elav-negative, Spa-positive cells comparing to control samples.

To understand if *stg* is required for the specification of R1 and R6, we can label L3 eye imaginal discs with Seven-up (Kramer *et al.*, 1995) or Bar (Higashijima *et al.*, 1992), which are exclusively expressed in these PR-cell types. Regarding to R7, the pattern of Pros was not conclusive (Figure 16 B, B'). However, we observed that upon *stg* downregulation PR-axons do not project into the medulla (Figure 20 B, B'), suggesting that R7 may not be specified upon *stg* downregulation. To address this question we can label L3 eye imaginal discs with Rh5 and Rh6 (Roignant & Treisman, 2009) or Sev (Tomlinson & Struhl, 2001), which are exclusively expressed by R7.

Overexpression of *stg* in PR-cells did not induce modifications on the adult retina pattern (Figure 13 B). However, the same parameters analyzed during larval stages upon *stg* downregulation (*e.g*. ommatidia organization, cytoskeleton, nuclei positioning) should be evaluated to confirm that high levels of Stg do not induce modifications in the developing eye.

4.2 *stg* is required for the apical maintenance of photoreceptor-nuclei

As referred above, upon *stg* downregulation PR-cells are not able to retain apically their nuclei (Figure 14 F'). Whited *et al.* (2004) showed that the maintenance of post-mitotic PR-nuclei depends on the balanced activities of dynactin and kinesin, which are responsible for the nuclei movement in the direction basal-to-apical and the opposed direction, respectively (Whited *et al.*, 2004). One hypothesis to explain the failure of PR-nuclei to maintain apically could be the requirement of Stg function for the activity of these motor

proteins. Indeed, several studies have reported that mutations in subunits of these proteins induce a strong displacement of PR-nuclei from their apical position. For instance, in mutants for the dynactin subunit Glued, kinesin heavy chain and for the dynein-associated protein Lis1, PR-nuclei have been detected along the OS and in the brain (Whited *et al.,* 2004). To understand if Stg interacts with these motor proteins we can perform genetic interactions using Elav-Gal4>*stg* RNAi flies and RNAi lines for dynein and kinesin components. If Stg directly interacts with Kinesin, upon downregulation we expect to see that PR-nuclei are maintained apically; if Stg interacts with Dynein, all nuclei will be retained basally upon its downregulation.

4.3 *stg* function is critical for cytoskeleton organization

Cytoskeleton is a crucial cell component that provides cellular shape and structural support during development. Both actin and MT cytoskeleton are regulated by actin and MT-associated proteins, which control the assembly and polymerization of MT and actin structures, ensuring their growth, maintenance and stability (reviewed in Dent *et al.,* 2011; Coles & Bradke, 2015). We observed that both actin and MT cytoskeleton become impaired upon *stg* downregulation: a disorganization of the structures and an abnormal accumulation of cytoskeletal proteins in the apical domain were detected (Figures 17 and 18, C-D'). These findings can be a sign that the function of these regulators is disrupted and hence, the normal cytoskeleton growth and dynamics is modified. This hypothesis is supported by results obtained through 2D-DIGE, where two actin regulators, Tropomyosin I and II, were detected as differentially expressed upon *stg* downregulation. These regulators are the main F-actin binding proteins responsible to stabilize actin filaments (Cooper, 2002; Gunning *et al.*, 2005).

Disruptions at the centrosome level might be another hypothesis to explain the cytoskeletal impairments observed. Centrosome is the major MT-organizing center composed by two centrioles surround by pericentriolar material, such as gamma-tubulin (Schiebel, 2000). Gamma-tubulin is required for the formation and function of the centrosome, where it is particularly important for MT nucleation, bipolar spindle formation and centriole duplication (Schiebel, 2000; Hughes *et al.*, 2011). Recent studies have reported an accumulation of gamma-tubulin at the centrosome upon proteasome inhibition (Zhao *et al.*, 2003). The functional link between proteasome activity and the centrosome is still unknown. More recently, Didier *et al.* (2008) demonstrated, using HeLa cells as a model, that the proteasome regulates centrosome proteins to maintain the proper function of

centrosome. When the proteasome activity was inhibited, an accumulation of pericentriolar proteins, such as gamma-tubulin, at the centrosome as observed. They concluded that this abnormal accumulation was due to an impaired MT nucleation and organization (Didier *et al.*, 2008). Taking this into account, the apical accumulation of Futsch and the failure to spread along the axons observed upon *stg* downregulation (Figure 18 C-D') could be due to an impairment at the centrosome or proteasome level. Several *Drosophila* RNAi lines for critical proteasome components were already generated: Rpn1, Rpn2, α5, β5 and β6 (Velentzas *et al.*, 2013). To test if Stg interacts with the proteasome machinery we can perform genetic interactions between these RNAi lines and Elav-Gal4>*stg* RNAi flies. If the interaction occurs we expect to see a greater accumulation of Futsch in L3 eye imaginal discs comparing to the observed in L3 eye disc of Elav-Gal4>*stg* RNAi.

4.4 *stg* is essential for axonal integrity and projection into the optic lobe

Upon *stg* downregulation we observed that PR-axons lost the homogeneous thin structure observed in control samples, acquiring a beads-like structure (swellings) (Figure 19 B-B''), which could be a consequence of the cytoskeletal impairments previously described. These axonal defects could impair the intracellular transport. Indeed, axonal swellings have been associated with alterations in MT dynamics and with an impaired axonal transport, supporting this hypothesis (Tarrade *et al.,* 2006). To demonstrated that the intracellular transport is impaired upon *stg* downregulation we can use L3 eye imaginal discs of the reporter line Elav-Gal4, UAS-syn::GFP, which expresses synaptotagmin as a GFP protein fusion. Since synaptotagmin is present in vesicles which are used to transport several cargos, with this approach we can analyze if the transport of these vesicles is disrupted. If *stg* downregulation disrupts the intracellular transport we expect to see an accumulation of vesicles at the cell body or basally. *In vivo* studies can also be performed to corroborate the observations and to access the vesicle traffic in PR-cells.

An impaired axonal transport could compromise the specification of lamina neurons, which requires incorrupt axons and a correct outgrowth to ensure the proper Hh transport into LPCs, located in the OL. To understand if lamina specification occurs properly upon *stg* downregulation we can label GMR-Gal4>*stg* RNAi L3 eye imaginal discs with Dac, which is expressed in differentiated lamina neurons (Mardon *et al.*, 1994). Elav-Gal4 is pan-neuronal, so it cannot be used to address this question. However, since GMR-Gal4 is expressed at the SMW, where some PR-cell types are generated, *stg* downregulation using

this driver will affect the formation of these PR-cells. Thus, there will be less PR-cells projecting to the OL and contributing to lamina differentiation. Nevertheless, this approach can be used to understand if lamina is or is not specified.

Upon *stg* downregulation we also detected that PR-axons fail to project into the medulla (Figure 20 B, B'). Among the eight PR-cells, only R7 and R8 project into this neuropil. If R7 is not properly specified upon *stg* downregulation, this could explain the absence of its projection into the medulla. R8 specification is not affected by *stg* downregulation. However, the cytoskeletal impairment and a defective axonal transport could be sufficient to perturb axon outgrowth. Glial cells are also involved in PR projection, guiding the developing axons into their targets. We analyzed glia migration into the eye imaginal disc and quantified the number of Repo-positive cells in control samples and upon *stg* downregulation. No significant difference was detected, suggesting that *stg* downregulation does not affect glia migration into the developing eye (Figures 26 and 27). Thereby, the impaired PR projection into the medulla may be independent of glia defects.

4.5 The potential link between Stg and neurodegeneration

The defects caused by *stg* downregulation during larval stages could lead to unstable PR-cells and consequently cell death. Several processes related to neuronal death, such as Caspase-3, Lamin and Cyclin B expression, and glia behavior were analyzed. Our results showed an abnormal accumulation of Cyclin in PR-cells, but neuronal death does not occur during L3.

4.5.1 Downregulation of *stg* induces an abnormal accumulation of Cyclin B in photoreceptors

At the end of mitosis, the APC/C promotes the degradation of mitotic cyclins, such as Cyc A and Cyc B, by the proteasome machinery (Sigrist & Lehner, 1997). In *Drosophila*, Fizzy-related (Fzr), the homologue of the Cdh1 regulatory subunit of the APC/C promotes the degradation of these mitotic cyclins (Sigrist & Lehner, 1997). Narbonne-Reveau *et al.* (2008) showed that compromising APC/C (Fzr/Cdh1) activity inhibits DNA replication and induces an accumulation of mitotic cyclins (Narbonne-Reveau *et al.*, 2008). Since upon *stg* downregulation we observed that posterior to the SMW some PR-cells accumulate Cyc B (Figure 23 C-D''), this could suggest a possible interaction between Stg and APC/C in order to promote de degradation of mitotic cyclins at the end of mitosis. Narbonne-Reveau *et al.*

(2008) also generated RNAi constructs for many critical APC/C subunits, such as Apc6, Apc8 and Apc10 (Narbonne-Reveau *et al.*, 2008). To evaluate this interaction we can perform genetic interactions between these RNAi lines and Elav-Gal4>*stg* RNAi flies. If a link between APC/C activity and Stg does exist, we expect to see a strong Cyc B accumulation in PR-cells posterior to the SMW.

The expression of mitotic cyclins such Cyc B in post-mitotic neurons has been correlated with a cell cycle re-entry (Busser *et al.*, 1998; Yang *et al.*, 2003). Thus, another hypothesis is that upon *stg* downregulation, PR-cells re-enter the cell cycle. To understand this question we can perform BrdU incorporation assay in L3 eye imaginal discs. If upon *stg* downregulation PR-cells are re-entering the cell cycle we expect to see BrdU incorporation in PR-cells localized posterior the SMW.

Okada *et al.* (2002) showed that in WT eye imaginal discs, *cyc B* mRNA is highly expressed anterior to the MF, while posteriorly this expression is reduced (Okada *et al.*, 2002). Thus, another hypothesis is that the accumulation of Cyc B may be a transcriptional defect caused by *stg* downregulation. To address this question we ca perform Real-Time PCR (RT-PCR) or an *in situ* hybridization for *cyc B* mRNA from L3 eye imaginal discs of Elav-Gal4 and Elav-Gal4>*stg* RNAi. If this hypothesis is true, we expected to see higher levels of *cyc B* mRNA in Elav-Gal4>*stg* RNAi comparing to Elav-Gal4.

4.5.2 Downregulation of *stg* does not induce photoreceptor cell death during larval stages

PPases are expressed in adult brains and play an essential role in several processes, such as neurogenesis and synaptic plasticity (reviewed in Tweedie-Cullen *et al.*, 2010). PPases have been associated with some neurodegenerative disorders, such as AD. High levels/activity of the mammalian CDC25s have been reported in AD brains and associated with cell cycle re-entry of post-mitotic neurons, inducing neuronal death (Chang *et al.*, 2012).

Our results show that *stg* downregulation impairs several structures and processes, including axonal organization/structure, nuclei positioning, axonal growth and transport, that could lead to unbalanced PR-cells and hence their cell death. However, we did not detect dying PR-cells during larval stages (Figures 24 and 25), which suggest that this process may only occur during pupa stages or adulthood. To confirm this hypothesis we can label eye imaginal discs from pupae with Elav and Caspase 3. If cell death occurs we expect to see Elav-positive, Caspase 3-positive cells.

4.5.3 *stg* downregulation does not promote changes in glia behavior

Glial cells are essential for the maintenance of a functional nervous system. In *Drosophila,* many glial defects have been described as responsible for late-onset neurodegeneration (Buchanan & Benzer, 1993; Kretzschmar *et al.*, 1997). One of these alterations is the overactivation, which promotes glia overmigration onto the eye imaginal disc (Yuva-Aydemir & Klämbt, 2011). We quantified the number of Repo-positive cells in the eye disc and no modifications were detected upon *stg* downregulation (Figures 26 and 27), which could suggest that *stg* downregulation does not induce glial defects and hence glia may be not contribute for the neurodegeneration observed.

4.6 2D-DIGE identified several potential neuronal-specific Stg substrates

2D-DIGE allow us to identify seven proteins which are differentially expressed upon *stg* downregulation (Figures 28 and 29). Among them, Tropomyosin I/II are strong substrates of Stg in post-mitotic neurons. Tropomyosin is the main actin-binding protein which regulated actin dynamics stabilizing actin filaments and inhibiting the activity of proteins which could destabilize actin filaments (*e.g.* cofilin) (Houle *et al.*, 2003). Tropomyosin is regulated by phosphorylation and when is dephosphorylated, the partially reconstituted actin filaments become disorganized (Rao *et al.*, 2009). As previously described, *stg* downregulation induces a slightly disorganization of F-actin and an apparent failure to localized along the axons (Figure 17 C-D'). Altogether, our findings suggest that Stg can interacts with Tropomyosin I/II in order to ensure a proper actin cytoskeleton organization during PR development. To ascertain this hypothesis (as well as for the other potential candidates identified) we need to perform genetic interactions between Elav-Gal4>*stg* RNAi flies and RNAi/UAS lines for Tropomyosin I/II. If the interaction occurs we expect to see a stronger phenotype than the observed in Elav-Gal4>*stg* RNAi flies.

5. Final remarks and future perspectives

5. FINAL REMARKS AND FUTURE PERSPECTIVES

Altogether, our results show that Stg phosphatase is required in the developing eye to ensure the highly organized retina pattern observed in adult flies. In this process, Stg could interact with several cell components in order to maintain the apical position of PR-nuclei but also to regulate both neuronal actin and MT cytoskeleton. Maintaining a highly coordination between actin and MT cytoskeleton dynamics, PR-axons acquire a regular and homogeneous axon structure, ensuring a proper intracellular transport, which will be important for the specification of lamina neurons, and survival of PR-cells. This coordinated activity will also be important for the proper axon extension into the lamina and medulla neuropils of the OL. Altogether, our work suggest that Stg phosphatase plays an essential role for the homeostasis of the *Drosophila* visual system neurons.

As a future work we will address in detail how does Stg activity contribute to the apical maintenance of PR-nuclei and cytoskeleton organization/dynamics. The potential neuronal substrates of Stg identified by 2D-DIGE will be validated through genetic interactions between Elav-Gal4>*stg* RNAi flies and RNAi/UAS lines for each candidate. Determine if Stg function is required during cell fate decisions and if its activity is important during adult stages are other interesting questions that we will analyze.

6. References

6. REFERENCES

Alphey, L. *et al.*, 1992. twine, a cdc25 homolog that functions in the male and female germline of drosophila. *Cell*, 69(6), pp.977–988.

Atkins, M. *et al.*, 2013. Dynamic Rewiring of the Drosophila Retinal Determination Network Switches Its Function from Selector to Differentiation. *PLoS Genetics*, 9(8), p.e1003731.

Avilés, E.C., Wilson, N.H. & Stoeckli, E.T., 2013. Sonic hedgehog and Wnt: antagonists in morphogenesis but collaborators in axon guidance. *Frontiers in Cellular Neuroscience*, 7, pp.1–17.

Baonza, A. & Freeman, M., 2005. Control of Cell Proliferation in the Drosophila Eye by Notch Signaling. *Developmental Cell*, 8(4), pp.529–539.

Baye, L.M. & Link, B.A., 2008. Nucelar migration during retinal development. *Brain Research*, 1192, pp.29–36.

Berger, C. *et al.*, 2007. The commonly used marker ELAV is transiently expressed in neuroblasts and glial cells in the Drosophila embryonic CNS. *Developmental Dynamics*, 236(12), pp.3562–3568.

Bessa, J. *et al.*, 2002. Combinatorial control of Drosophila eye development by Eyeless, Homothorax, and Teashirt. *Genes & Development*, 16(18), pp.2415–2427.

Boutros, R., Lobjois, V. & Ducommun, B., 2007. CDC25 phosphatases in cancer cells: key players? Good targets? *Nature reviews. Cancer*, 7(7), pp.495–507.

Brand, A H. & Dormand, E.L., 1995. the Gal4 System As a Tool for Unraveling the Mysteries of the Drosophila Nervous-System. *Current Opinion in Neurobiology*, 5(5), pp.572–578.

Brand, A.H. & Perrimon, N., 1993. Targeted gene expression as a means of altering cell fates and generating dominant phenotypes. *Development (Cambridge, England)*, 118(2), pp.401–15.

Buchanan, R.L. & Benzer, S., 1993. Defective Glia in the Drosophila Brain Degeneration Mutant drop-dead. *Neuron*, 10(5), pp.839–850.

Buendia, B., Santa-Maria, A. & Courvalin, J.C., 1999. Caspase-dependent proteolysis of integral and peripheral proteins of nuclear membranes and nuclear pore complex proteins during apoptosis. *Journal of cell science*, 112(11), pp.1743–53.

Busino, L. *et al.*, 2004. Cdc25A phosphatase: combinatorial phosphorylation, ubiquitylation and proteolysis. *Oncogene*, 23(11), pp.2050–2056.

Busser, J., Geldmacher, D.S. & Herrup, K., 1998. Ectopic Cell Cycle Proteins Predict the Sites of

Neuronal Cell Death in Alzheimer's Disease Brain. *J. Neurosci.*, 18(8), pp.2801–2807.

Cagan, R., 2009. Principles of Drosophila eye differentiation. *Current topics in developmental biology*, 89, pp.115–35.

Campos-Ortega, J. A. & Hartenstein, V., 1997. The Embryonic Development of Drosophila melanogaster. In *Springer-Verlag Berlin*. pp. 1–405.

Carthew, R.W., 2007. Pattern formation in the Drosophila eye. *Current opinion in genetics & development*, 17(4), pp.309–313.

Chang, H.C. *et al.*, 1995. phyllopod functions in the fate determination of a subset of photoreceptors in Drosophila. *Cell*, 80(3), pp.463–72.

Chang, K.H., Vincent, F. & Shah, K., 2012. Deregulated Cdk5 Triggers Aberrant Activation of Cell Cycle Kinases and Phosphatases Inducing Neuronal Death. *Journal of Cell Science*, 125(11), pp.5124–5137.

Charlton-Perkins, M. *et al.*, 2011. Prospero and Pax2 combinatorially control neural cell fate decisions by modulating Ras- and Notch-dependent signaling. *Neural Development*, 6(1), p.20.

Chevalier-Larsen, E. & Holzbaur, E.L.F., 2006. Axonal transport and neurodegenerative disease. *Biochimica et Biophysica Acta (BBA) - Molecular Basis of Disease*, 1762(11-12), pp.1094–1108.

Choi, K.W. & Benzer, S., 1994. Migration of glia along photoreceptor axons in the developing drosophila eye. *Neuron*, 12(2), pp.423–431.

Chotard, C., Leung, W. & Salecker, I., 2005. glial cells missing and gcm2 Cell Autonomously Regulate Both Glial and Neuronal Development in the Visual System of Drosophila. *Neuron*, 48(2), pp.237–251.

Clandinin, T.R. & Zipursky, S.L., 2002. Making connections in the fly visual system. *Neuron*, 35(5), pp.827–841.

Coles, C.H. & Bradke, F., 2015. Coordinating Neuronal Actin – Microtubule Dynamics. *Current Biology*, 25(15), pp.R677–R691.

Cooper, J.A., 2002. Actin dynamics: tropomyosin provides stability. *Current biology : CB*, 12(15), pp.R523–5.

Crew, J.R., Batterham, P. & Pollock, J. A., 1997. Developing compound eye in lozenge mutants of

Drosophila : lozenge expression in the R7 equivalence group. *Development Genes and Evolution*, 206(8), pp.481–493.

Czerny, T. *et al.*, 1999. Twin of eyeless, a second Pax-6 gene of Drosophila, acts upstream of eyeless in the control of eye development. *Molecular Cell*, 3(3), pp.297–307.

Debasish, P. *et al.*, 2013. Mass Spectrometry based Proteomics in Molecular Diagnostics: Discovery of Cancer Biomarkers using Tissue Culture. *Downloads.Hindawi.Com*, 2013, p.16.

Demerec, M. & Kaufman, B.P., 1996. *Drosophila guide* Carnegie I., Washington.

Dent, E.W. & Gertler, F.B., 2003. Cytoskeletal dynamics and transport in growth cone motility and guidance. *Neuron*, 40(2), pp.209–227.

Dent, E.W., Gupton, S.L. & Gertler, F.B., 2011. The growth cone cytoskeleton in Axon outgrowth and guidance. *Cold Spring Harbor Perspectives in Biology*, 3(3), pp.1–39.

Dickson, B.J. *et al.*, 1995. Control of Drosophila photoreceptor cell fates by phyllopod, a novel nuclear protein acting downstream of the Raf kinase. *Cell*, 80, pp.453–462.

Didier, C. *et al.*, 2008. Inhibition of proteasome activity impairs centrosome-dependent microtubuel nucleation and organization. *Molecular biology of the cell*, 19(3), pp.1220–1229.

Dokucu, M.E., Zipursky, S.L. & Cagan, R.L., 1996. Atonal, rough and the resolution of proneural clusters in the developing Drosophila retina. *Development (Cambridge, England)*, 122(12), pp.4139–4147.

Domingos, P.M. *et al.*, 2004. Spalt transcription factors are required for R3/R4 specification and establishment of planar cell polarity in the Drosophila eye. *Development (Cambridge, England)*, 131(22), pp.5695–5702.

Domínguez, M., 1999. Dual role for Hedgehog in the regulation of the proneural gene atonal during ommatidia development. *Development (Cambridge, England)*, 126(11), pp.2345–2353.

Domínguez, M. & Hafen, E., 1997. Hedgehog directly controls initiation and propagation of retinal differentiation in the Drosophila eye. *Genes & development*, 11(23), pp.3254–64.

Duffy, J.B., 2002. GAL4 system in Drosophila: a fly geneticist's Swiss army knife. *Genesis (New York, N.Y. : 2000)*, 34(1-2), pp.1–15.

Fan, S.S. & Ready, D.F., 1997. Glued participates in distinct microtubule-based activities in Drosophila eye development. *Development (Cambridge, England)*, 124(8), pp.1497–507.

6. REFERENCES

Ferguson, A.M. *et al.*, 2005. Normal Cell Cycle and Checkpoint Responses in Mice and Cells Lacking Cdc25B and Cdc25C Protein Phosphatases. *Society*, 25(7), pp.2853–2860.

Ferguson, K.L. *et al.*, 2005. A cell-autonomous requirement for the cell cycle regulatory protein, Rb, in neuronal migration. *The EMBO journal*, 24(24), pp.4381–91.

Fischbach, K.F. & Dittrich, P., 1989. The optic lobe of Drosophila melanogaster. I: A. Golgi analysis of wild-type structure. *Cell Tissue Res*, 258, pp.441–475.

Frank, C.L. & Tsai, L.H., 2013. Alternative functions of core cell cycle regulators in neuronal migration, neuronal maturation, and synaptic plasticity. , 18(9), pp.1199–1216.

Frank, C.L. & Tsai, L.H., 2009. Alternative Functions of Core Cell Cycle Regulators in Neuronal Migration, Neuronal Maturation, and Synaptic Plasticity. *Neuron*, 62(3), pp.312–326.

Frankfort, B.J. & Mardon, G., 2002. R8 development in the Drosophila eye: a paradigm for neural selection and differentiation. *Development (Cambridge, England)*, 129(6), pp.1295–1306.

Freeman, M., 1996. Reiterative use of the EGF receptor triggers differentiation of all cell types in the Drosophila eye. *Cell*, 87(4), pp.651–660.

Freeman, M., Kimmel, B.E. & Rubin, G.M., 1992. Identifying targets of the rough homeobox gene of Drosophila: evidence that rhomboid functions in eye development. *Development (Cambridge, England)*, 116(2), pp.335–346.

Fu, W. & Baker, N.E., 2003. Deciphering synergistic and redundant roles of Hedgehog, Decapentaplegic and Delta that drive the wave of differentiation in Drosophila eye development. *Development*, 130(21), pp.5229–5239.

Fu, W. & Noll, M., 1997. The Pax2 homolog sparkling is required for development of cone and pigment for development of cone and pigment for development of cone and cells in the Drosophila eye. *Denes Development*, 11(16), pp.2066–2078.

Gabrielli, B.G. *et al.*, 1996. Cytoplasmic accumulation of cdc25B phosphatase in mitosis triggers centrosomal microtubule nucleation in HeLa cells. *Journal of cell science*, 109(5), pp.1081–93.

Galaktionov, K. & Beach, D., 1991. Specific activation of cdc25 tyrosine phosphatases by B-type cyclins: Evidence for multiple roles of mitotic cyclins. *Cell*, 67(6), pp.1181–1194.

Gavet, O. & Pines, J., 2010. Activation of cyclin B1-Cdk1 synchronizes events in the nucleus and the cytoplasm at mitosis. *The Journal of Cell Biology*, 189(2), pp.247–259.

Greenwood, S. & Struhl, G., 1999. Progression of the morphogenetic furrow in the Drosophila eye: the roles of Hedgehog, Decapentaplegic and the Raf pathway. *Development (Cambridge, England)*, 126(24), pp.5795–5808.

Gunning, P.W. *et al.*, 2005. Tropomyosin isoforms: Divining rods for actin cytoskeleton function. *Trends in Cell Biology*, 15(6), pp.333–341.

Hadjieconomou, D., Timofeev, K. & Salecker, I., 2011. A step-by-step guide to visual circuit assembly in Drosophila. *Current Opinion in Neurobiology*, 21(1), pp.76–84.

Halter, D. A *et al.*, 1995. The homeobox gene repo is required for the differentiation and maintenance of glia function in the embryonic nervous system of Drosophila melanogaster. *Development (Cambridge, England)*, 121(2), pp.317–332.

Hart, A.C. *et al.*, 1990. Induction of cell fate in the Drosophila retina: the bride of sevenless protein is predicted to contain a large extracellular domain and seven transmembrane segments. *Genes & development*, 4(11), pp.1835–47.

Harte, P.J. & Kankel, D.R., 1983. Analysis of visual system development in Drosophila melanogaster: Mutations at the Glued locus. *Developmental Biology*, 99(1), pp.88–102.

Heberlein, U. & Moses, K., 1995. Mechanisms of Drosophila retinal morphogenesis: The virtues of being progressive. *Cell*, 81(7), pp.987–990.

Heberlein, U., Wolff, T. & Rubin, G.M., 1993. The TGF-beta homolog dpp and the segment polarity gene hedgehog are required for propagation of a morphogenetic wave in the Drosophila retina. *Cell*, 75(5), pp.913–926.

Herrup, K. & Yang, Y., 2007. Cell cycle regulation in the postmitotic neuron: oxymoron or new biology? *Nature reviews. Neuroscience*, 8(5), pp.368–378.

Higashijima, S.I. *et al.*, 1992. Dual Bar homeo box genes of Drosophila required in two photoreceptor cells, R1 and R6, and primary pigment cells for normal eye development. *Genes and Development*, 6(1), pp.50–60.

Hirokawa, N. & Takemura, R., 2004. Molecular motors in neuronal development, intracellular transport and diseases. *Current Opinion in Neurobiology*, 14(5), pp.564–573.

Hoffmann, I. *et al.*, 1993. Phosphorylation and activation of human cdc25-C by cdc2--cyclin B and its involvement in the self-amplification of MPF at mitosis. *The EMBO journal*, 12(1), pp.53–63.

Houle, F. *et al.*, 2003. Extracellular signal-regulated kinase mediates phosphorylation of

Tropomyosin-1 to promote cytoskeleton remodeling in response to oxidative stress: impact on membrane blebbing. *Molecular biology of the cell*, 14(4), pp.1418–32.

Hughes, S.E. *et al.*, 2011. Gamma-tubulin is required for bipolar spindle assembly and for proper kinetochore microtubule attachments during prometaphase I in Drosophila oocytes. *PLoS genetics*, 7(8), p.e1002209.

Hurd, D.D. & Saxton, W.M., 1996. Kinesin mutations cause motor neuron disease phenotypes by disrupting fast axonal transport in Drosophila. *Genetics*, 144(3), pp.1075–85.

Husseman, J.W., Nochlin, D. & Vincent, I., 2000. Mitotic activation: a convergent mechanism for a cohort of neurodegenerative diseases. *Neurobiology of aging*, 21(6), pp.815–28.

Jennings, B.H., 2011. Drosophila-a versatile model in biology & medicine. *Materials Today*, 14(5), pp.190–195.

Karlsson-Rosenthal, C. & Millar, J.B.A., 2006. Cdc25: mechanisms of checkpoint inhibition and recovery. *Trends in Cell Biology*, 16(6), pp.285–292.

Kauffmann, R.C. *et al.*, 1999. Ras1 signaling and transcriptional competence in the R7 cell of Drosophila. *Genes and Development*, 10(17), pp.2167–2178.

Kim, A.H. *et al.*, 2009. A centrosomal Cdc20-APC pathway controls dendrite morphogenesis in postmitotic neurons. , 130(29), pp.9492–9499.

Kimmel, B.E., Heberlein, U. & Rubin, G.M., 1990. The homeo domain protein rough is expressed in a subset of cells in the developing Drosophila eye where it can specify photoreceptor cell subtype. *Genes & development*, 4(5), pp.712–27.

Kramer, S., West, S.R. & Hiromi, Y., 1995. Cell fate control in the Drosophila retina by the orphan receptor seven-up: its role in the decisions mediated by the ras signaling pathway. *Development (Cambridge, England)*, 121(5), pp.1361–72.

Kretzschmar, D. *et al.*, 1997. The swiss cheese mutant causes glial hyperwrapping and brain degeneration in Drosophila. *The Journal of neuroscience : the official journal of the Society for Neuroscience*, 17(19), pp.7425–7432.

Krohne, G. & Benavente, R., 1986. The nuclear lamins: a multigene family of proteins in evolution and differentiation. *Experimental Cell Research*, 162(1), pp.1–10.

Lammer, C. *et al.*, 1998. The cdc25B phosphatase is essential for the G2/M phase transition in human cells. *Journal of cell science*, 111(16), pp.2445–53.

Leavens, D. A., 2007. Microtubule polymerization: one step at a time. *Current Biology*, 17(17), pp.764–766.

Lee, C.H. *et al.*, 2001. N-cadherin regulates target specificity in the Drosophila visual system. *Neuron*, 30(2), pp.437–450.

Lehman, D. A *et al.*, 1999. Cis-regulatory elements of the mitotic regulator, string/Cdc25. *Development (Cambridge, England)*, 126(9), pp.1793–1803.

Lim, J. & Choi, K.-W., 2003. Bar homeodomain proteins are anti-proneural in the Drosophila eye: transcriptional repression of atonal by Bar prevents ectopic retinal neurogenesis. *Development (Cambridge, England)*, 130(24), pp.5965–74.

Lim, J. & Choi, K.-W., 2004. Induction and autoregulation of the anti-proneural gene Bar during retinal neurogenesis in Drosophila. *Development (Cambridge, England)*, 131(22), pp.5573–80.

Lindqvist, A. *et al.*, 2005. Cdc25B cooperates with Cdc25A to induce mitosis but has a unique role in activating cyclin B1-Cdk1 at the centrosome. *The Journal of cell biology*, 171(1), pp.35–45.

Lopes, C.S. & Casares, F., 2010. hth maintains the pool of eye progenitors and its downregulation by Dpp and Hh couples retinal fate acquisition with cell cycle exit. *Developmental Biology*, 339(1), pp.78–88.

Ma, C. *et al.*, 1993. The segment polarity gene hedgehog is required for progression of the morphogenetic furrow in the developing Drosophila eye. *Cell*, 75(5), pp.927–938.

Manfredi, G. & Xu, Z., 2005. Mitochondrial dysfunction and its role in motor neuron degeneration in ALS. *Mitochondrion*, 5(2), pp.77–87.

Mardon, G., Solomon, N.M. & Rubin, G.M., 1994. dachshund encodes a nuclear protein required for normal eye and leg development in Drosophila. *Development (Cambridge, England)*, 120(12), pp.3473–3486.

Martin, M. *et al.*, 1999. Cytoplasmic dynein, the dynactin complex, and kinesin are interdependent and essential for fast axonal transport. *Molecular biology of the cell*, 10(11), pp.3717–28.

Morante, J. & Desplan, C., 2013. The color vision circuit in the medulla of Drosophila. , 18(9), pp.1199–1216.

Morante, J., Desplan, C. & Celik, A., 2007. Generating patterned arrays of photoreceptors. *Curr Opin Genet Dev*, 17(4), pp.314–319.

Morin, X. *et al.*, 2001. A protein trap strategy to detect GFP-tagged proteins expressed from their endogenous loci in Drosophila. *Proceedings of the National Academy of Sciences of the United States of America*, 98(26), pp.15050–15055.

Morris, R.L. & Hollenbeck, P.J., 1993. The regulation of bidirectional mitochondrial transport is coordinated with axonal outgrowth. *Journal of cell science*, 104(3), pp.917–927.

Mozer, B. A & Easwarachandran, K., 1999. Pattern formation in the absence of cell proliferation: tissue-specific regulation of cell cycle progression by string (stg) during Drosophila eye development. *Developmental biology*, 213(1), pp.54–69.

Murciano, A. *et al.*, 2002. Interkinetic Nuclear Movement May Provide Spatial Clues to the Regulation of Neurogenesis. *Molecular and Cellular Neuroscience*, 21(2), pp.285–300.

Narbonne-Reveau, K. *et al.*, 2008. APC/CFzr/Cdh1 promotes cell cycle progression during the Drosophila endocycle. *Development*, 135(8), pp.1451–1461.

Nguyen, L. *et al.*, 2007. p27 (kip1) independently promotes neuronal differentiation and migration in the cerebral cortex. *Bull Mem Acad R Med Belg*, 162(5-6), pp.310–4.

Norden, C. *et al.*, 2009. Actomyosin Is the Main Driver of Interkinetic Nuclear Migration in the Retina. *Cell*, 138(6), pp.1195–1208.

O'Farrell, P.H., 1975. High Resolution Two-Dimensional Eçectrophoresis of proteins. *The Journal of Biological Chemistry*, 250(10), pp.4007–4021.

Okada, M. *et al.*, 2002. Myb controls G2/M progression by inducing cyclin B expression in the Drosophila eye imaginal disc. *EMBO Journal*, 21(4), pp.675–684.

Pappu, K.S., 2003. Mechanism of hedgehog signaling during Drosophila eye development. *Development*, 130(13), pp.3053–3062.

Pielage, J. *et al.*, 2003. The drosophila cell survival gene discs lost encodes a cytoplasmic codanin-1-like protein, not a homolog of tight junction PDZ protein Patj. *Developmental Cell*, 5(6), pp.841–851.

Pinto, S. *et al.*, 1999. Latheo Encodes a Subunit of the Origin Recognition Complex and Disrupts Neuronal Proliferation and Adult Olfactory Memory When Mutant. *Neuron*, 23(1), pp.45–54.

Poeck, B. *et al.*, 2001. Glial cells mediate target layer selection of retinal axons in the developing visual system of Drosophila. *Neuron*, 29(1), pp.99–113.

Prokop, A. *et al.*, 2013. Using fly genetics to dissect the cytoskeletal machinery of neurons during

axonal growth and maintenance. *Journal of cell science*, 126(11), pp.2331–41.

Rao, V.S., Marongelli, E.N. & Guilford, W.H., 2009. Phosphorylation of Tropomyosin extends cooperative binding of myosin beyond a single regulatory unit. *Cell Motil Cytos*, 66(1), pp.10–23.

Ready, D.F., Hanson, T.E. & Benzer, S., 1976. Development of the Drosophila retina, a neurocrystalline lattice. *Developmental Biology*, 53(2), pp.217–240.

Riedl, J. *et al.*, 2008. Lifeact: a versatile marker to visualize F-actin. *Nat Methods*, 5(7), pp.1–8.

Roignant, J. & Treisman, J., 2009. Pattern formation in Drosophila eye disc. *Int J Dev Biol*, 53(5-6), pp.795–804.

Russell, P. & Nurse, P., 1986. cdc25+ functions as an inducer in the mitotic control of fission yeast. *Cell*, 45(1), pp.145–153.

Sabry, J.H. *et al.*, 1991. Microtubule behavior during guidance of pioneer neuron growth cones in situ. *Journal of Cell Biology*, 115(2), pp.381–395.

Sanes, J. & Zipursky, S., 2010. Design principles of insect and vertebrate visual systems. *Neuron*, 66(1), pp.15–36.

Schenk, J. *et al.*, 2009. Myosin II is required for interkinetic nuclear migration of neural progenitors. *Proceedings of the National Academy of Sciences of the United States of America*, 106(38), pp.16487–92.

Schiebel, E., 2000. gamma-tubulin complexes: Binding to the centrosome, regulation and microtubule nucleation. *Current Opinion in Cell Biology*, 12(1), pp.113–118.

Schuldiner, O. *et al.*, 2009. piggyBac-based mosaic screen identifies a postmitotic function for cohesin in regulating developmental axon pruning. , 14(2), pp.227–238.

Shaham, S., 2005. Glia–Neuron Interactions in Nervous System Function and Development. , 69(1846), pp.39–66.

Shi, Y. & Noll, M., 2009. Determination of cell fates in the R7 equivalence group of the Drosophila eye by the concerted regulation of D-Pax2 and TTK88. *Developmental Biology*, 331(1), pp.68–77.

Shinza-Kameda, M. *et al.*, 2006. Regulation of layer-specific targeting by reciprocal expression of a cell adhesion molecule, Capricious. *Neuron*, 49(2), pp.205–213.

Sigrist, S.J. & Lehner, C.F., 1997. Drosophila fizzy-related down-regulates mitotic cyclins and is

required for cell proliferation arrest and entry into endocycles. *Cell*, 90(4), pp.671–681.

Silies, M. & Klämbt, C., 2010. APC/CFzr/Cdh1-dependent regulation of cell adhesion controls glial migration in the Drosophila PNS. *Nature Neuroscience*, 13(11), pp.1357–1364.

Simon, M.A., 1994. Signal transduction during the development of the Drosophila R7 photoreceptor. *Developmental biology*, 166(2), pp.431–42.

Sink, H. *et al.*, 2001. Sidestep encodes a target-derived attractant essential for motor axon guidance in Drosophila. *Cell*, 105(1), pp.57–67.

Suzumura, A. *et al.*, 2006. Roles of glia-derived cytokines on neuronal degeneration and regeneration. *Ann N Y Acad Sci*, 1088, pp.219–29.

Tarrade, A. *et al.*, 2006. A mutation of spastin is responsible for swellings and impairment of transport in a region of axon characterized by changes in microtubule composition. *Human molecular genetics*, 15(24), pp.3544–58.

Taverna, E. & Huttner, W.B., 2010. Neural progenitor nuclei IN motion. *Neuron*, 67(6), pp.906–914.

Thomas, B., 1994. Cell cycle progression in the developing Drosophila eye: roughex encodes a novel protein required for the establishment of G1. *Cell*, 77(7), pp.1003–1014.

Tomasi, T. *et al.*, 2008. The Transmembrane Protein Golden Goal Regulates R8 Photoreceptor Axon-Axon and Axon-Target Interactions. *Neuron*, 57(5), pp.691–704.

Tomlinson, A. & Ready, D.F., 1987. Neuronal differentiation in the Drosophila ommatidium. *Developmental Biology*, 120(2), pp.366–376.

Tomlinson, A. & Struhl, G., 2001. Delta/Notch and Boss/Sevenless signals act combinatorially to specify the Drosophila R7 photoreceptor. *Mol Cell*, 7(3), pp.487–495.

Treisman, J.E., 2013. Retinal differentiation in Drosophila. *Wiley Interdisciplinary Reviews: Developmental Biology*, 2(4), pp.545–557.

Tweedie-Cullen, Y., Park, C.S. & Mansuy, I.M., 2010. Protein phosphatases in the brain: regulation, function and disease. In *Protein Reviews*. pp. 233–257.

Velentzas, P.D. *et al.*, 2013. Proteasome, but not autophagy, disruption results in severe eye and wing dysmorphia: a subunit- and regulator-dependent process in Drosophila. *PloS one*, 8(11), p.e80530.

Welte, M.A., 2004. Bidirectional Transport along Microtubules. *Current Biology*, 14(13),

pp.R525–R537.

Whited, J.L. *et al.*, 2004. Dynactin is required to maintain nuclear position within postmitotic Drosophila photoreceptor neurons. *Development (Cambridge, England)*, 131(19), pp.4677–4686.

Wolff, T. & Ready, D.F., 1991. The beginning of pattern formation in the Drosophila compound eye: the morphogenetic furrow and the second mitotic wave. *Development (Cambridge, England)*, 113(3), pp.841–50.

Yang, Y., Geldmacher, D.S. & Herrup, K., 2001. DNA replication precedes neuronal cell death in Alzheimer's disease. *The Journal of neuroscience : the official journal of the Society for Neuroscience*, 21(8), pp.2661–8.

Yang, Y., Mufson, E.J. & Herrup, K., 2003. Neuronal cell death is preceded by cell cycle events at all stages of Alzheimer's disease. *The Journal of neuroscience : the official journal of the Society for Neuroscience*, 23(7), pp.2557–2563.

Yuva-Aydemir, Y., Bauke, A.-C. & Klämbt, C., 2011. Spinster controls Dpp signaling during glial migration in the Drosophila eye. *The Journal of neuroscience : the official journal of the Society for Neuroscience*, 31(19), pp.7005–7015.

Yuva-Aydemir, Y. & Klämbt, C., 2011. Long-range signaling systems controlling glial migration in the Drosophila eye. *Developmental Neurobiology*, 71(12), pp.1310–1316.

Zhang, T. *et al.*, 2006. Direct control of neurogenesis by selector factors in the fly eye: regulation of atonal by Ey and So. *Development*, 133(24), pp.4881–4889.

Zhao, J. *et al.*, 2003. Parkin is recruited to the centrosome in response to inhibition of proteasomes. *Journal of cell science*, 116(19), pp.4011–9.